Introduction and HVP dispersive contribution to the muon g-2 prediction

Michel Davier

Laboratoire Irène Joliot-Curie (IJCLab) –CNRS/IN2P3 et Université Paris-Saclay

- April 7 2021: announcement of the first result of the Fermilab experiment measuring the muon magnetic anomaly

- Comparison with the theoretical prediction within the Standard Model shows an excess at the level of 4.2 σ, larger than the previous 3.7 σ with respect to the Brookhaven experiment

- In this talk, after a general introduction and some information on the experiment, I will review the status of the hadronic vacuum polarization contribution using a dispersion relation based on the measured cross sections for e+ e- $\rightarrow$ hadrons

The electron g-2 early history

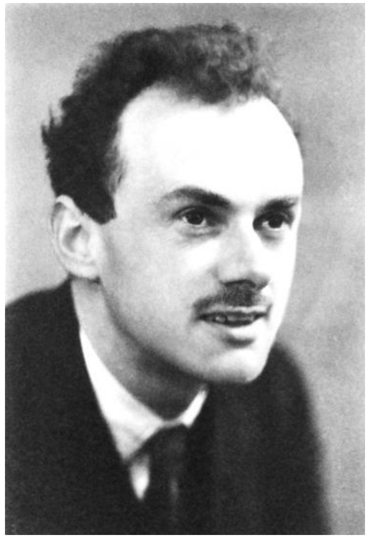

- Dirac's relativistic theory of the electron (1928) naturally accounted for quantized particle spin, and described elementary spin-1/2 particles (and their anti-particles)

- In the classical limit, one finds the Pauli equation with a magnetic moment:

$$\vec{\mu} = -g_e \frac{e}{2m_e} \vec{S}$$ with $|\boldsymbol{g_e}| = 2$ is **the gyromagnetic factor**

- Dirac's prediction was confirmed to 0.1% by Kinsler & Houston in 1934 through studying the Zeeman effect in neon

- A deviation from $g_e = 2$ was established by Nafe, Nels & Rabi only in 1947 by comparing the hyperfine structure of hydrogen and deuterium spectra

- A first precision measurement of $g_e = 2.00344 \pm 0.00012$ (*wrong: 2.00232…*!) was made by Kusch & Foley in 1947 using Rabi's atomic beam magnetic resonance technique

- Why does g_e deviate from 2 at 10^{-3} level ? (new physics?)

magnetic anomaly a = (g–2) / 2

Quantum field theory

- Development of quantum electrodynamics (Dyson, Feynman, Schwinger, Tomonaga) : emission/absorption of photons by electrons implies quantum fluctuations (virtual particles), divergences are regularized by renormalization. Amplitude for any QED process written as a perturbative expansion in the coupling constant e (visualized with Feynman diagrams for any order)

- Dirac's g = 2 corresponds to the lowest order QED graph

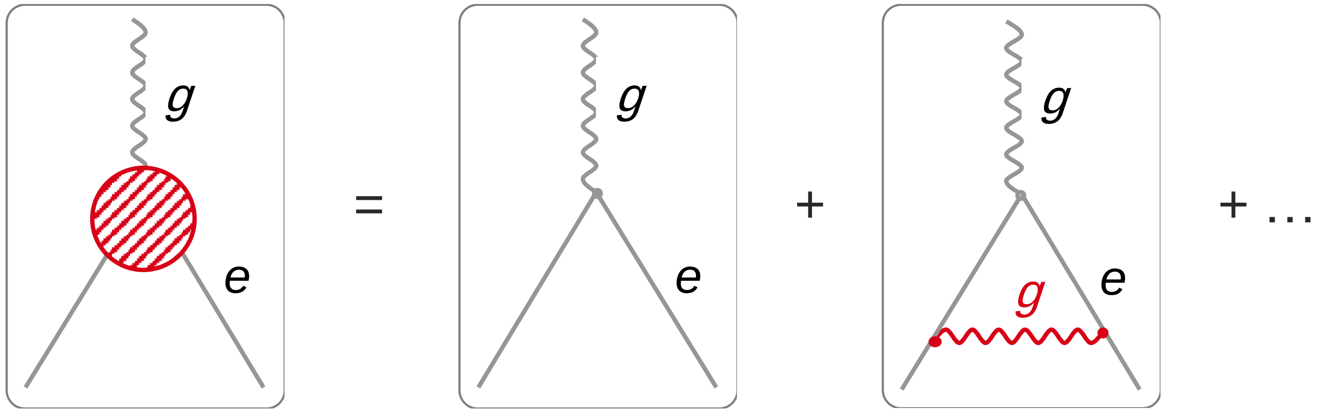

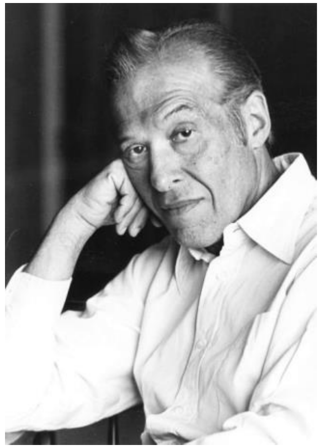

- First correction (order α) computed by Schwinger in 1948, in agreement with the experimental anomaly

$$a_e^{\mathrm{QED}} = \frac{\alpha}{2\pi} + \cdots = 0.001\,161\ \ldots$$

- As precision improved: necessity to include higher-order QED terms, as well as contributions from other known interactions and possibly beyond what we know

Why measure the muon g-2 ?

- 3 families of fermions (leptons and quarks) with universal coupling strengths to electroweak interactions
- The 3 charged leptons $l \equiv (e, \mu, \tau)$ differ only by their own leptonic quantum numbers and their masses

  m_e = 0.511 MeV m_μ = 105.7 MeV m_τ = 1776.9 MeV
- e stable, μ and τ are unstable and decay through the weak interaction with lifetimes 2.2 μs and 390 fs

- sensitivity of a_l to new physics at energy scale Λ goes like m_l^2 / Λ^2
- Muon more sensitive by large factor $(m_\mu / m_e)^2 \sim 43000$, but measurement limited by short lifetime
- Measurement for τ lepton not practical at the moment

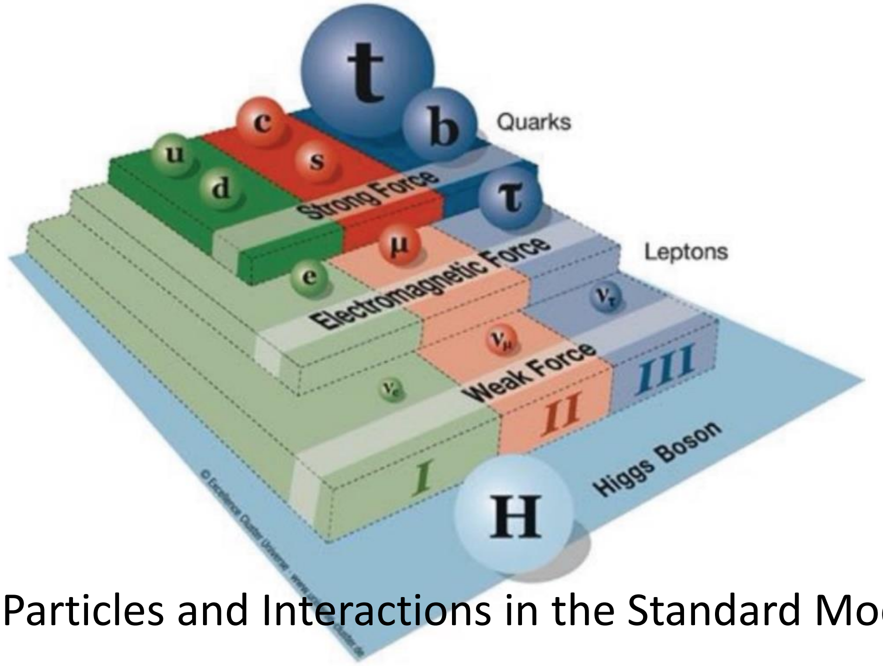

Particles and Interactions in the Standard Model

Key ingredients for measurement: polarized muons and muon spin analysis through decay electrons, both following from maximum P violation in weak interaction

- Muons produced at accelerators by pion decay are polarized

- Angle of energetic decay electrons are correlated with muon spin

Principle of muon g-2 measurement (CERN 1960-80)

spin orientation

$$\bar{\nu}_\mu \longleftarrow \pi^- \longrightarrow \mu^-_{\text{polarized}}$$

1. Parity violation polarizes muons in pion decay

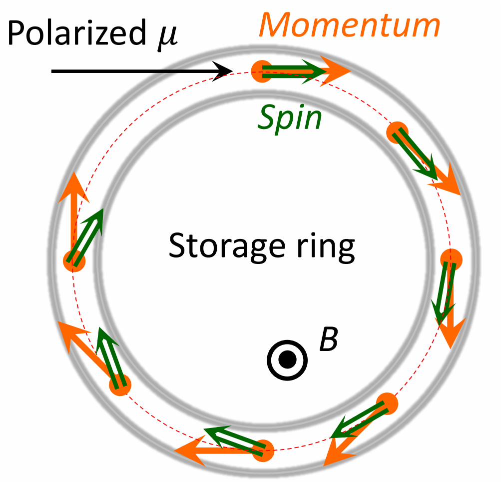

2. Anomalous frequency proportional to a_μ

- Very uniform magnetic field
- Focusing with electrostatic quadrupoles

3. Magic γ to cancel $\beta \times E$ effect:

$$\vec{\omega}_a = \frac{e}{m_\mu c}\left[a_\mu \vec{B} - \left(a_\mu - \frac{1}{\gamma^2 - 1}\right)\vec{\beta} \times \vec{E}\right] \approx \frac{e}{m_\mu c} a_\mu \vec{B}$$

P_μ = 3.09 GeV/c

4. Again parity violation in muon decay

$$\mu^-_{\text{polarized}} \longrightarrow e^- + \bar{\nu}_e + \nu_\mu$$

fast electron emitted in direction opposite to muon spin

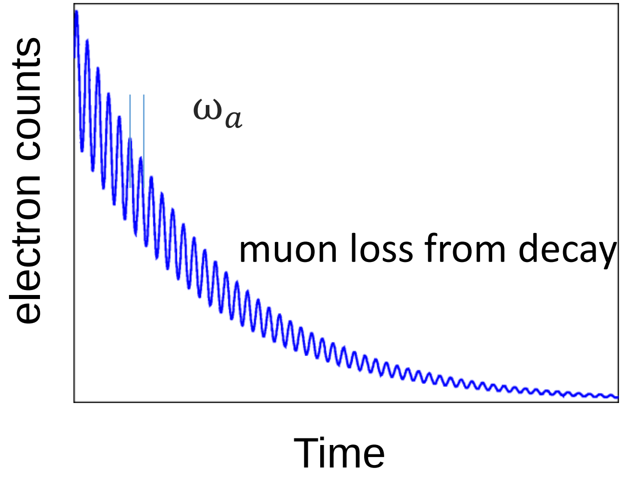

Double miracle by virtue of P violation !

Muon g-2 measurement (Brookhaven 1990-2006)

- A 24 GeV proton beam (AGS) incident on a target produces large number of pions that decay to muons
- The 3.1 GeV muon beam (relativistically enhanced lifetime of 64 μs) is injected into a 7.1 m radius ring with 1.4 T vertical magnetic field, which produces cyclotron motion matching the ring radius
- Electrostatic focusing of the beam is provided by a series of quadrupole lenses around the ring.

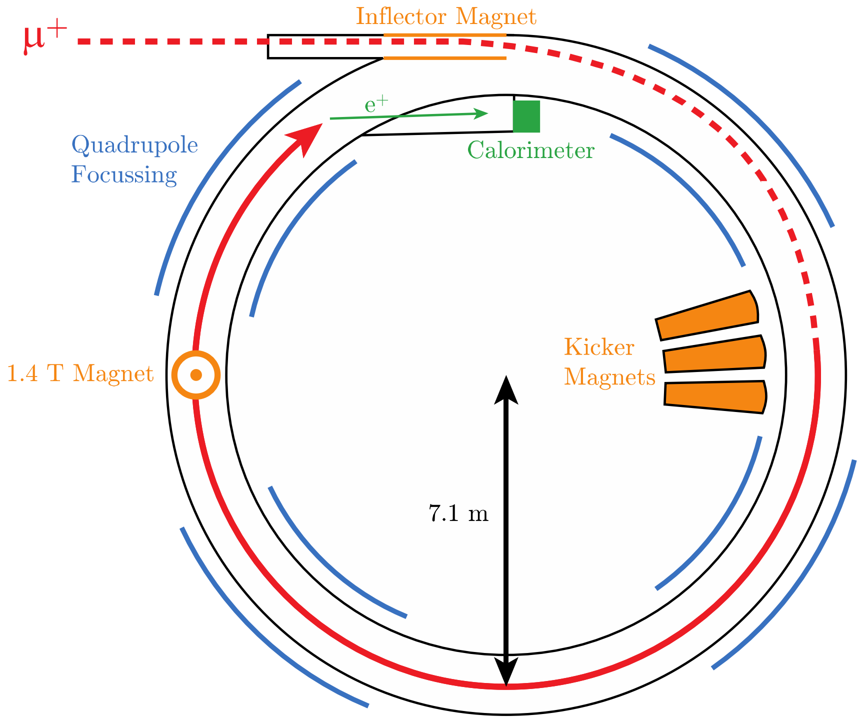

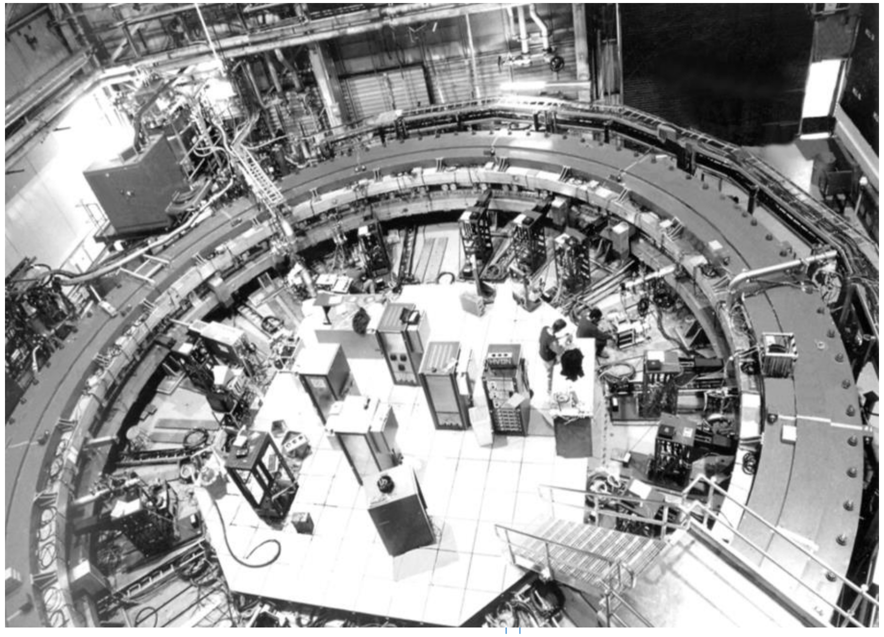

- Decay electrons (correlated with μ spin precession) counted vs. time in calorimeters inside ring ($\rightarrow \omega_a$)
- Precise measurement of ω_a and B allows to extract a_μ

Muon g-2 measurement (Brookhaven 1990-2006)

E821 (g –2), hep-ex/0202024

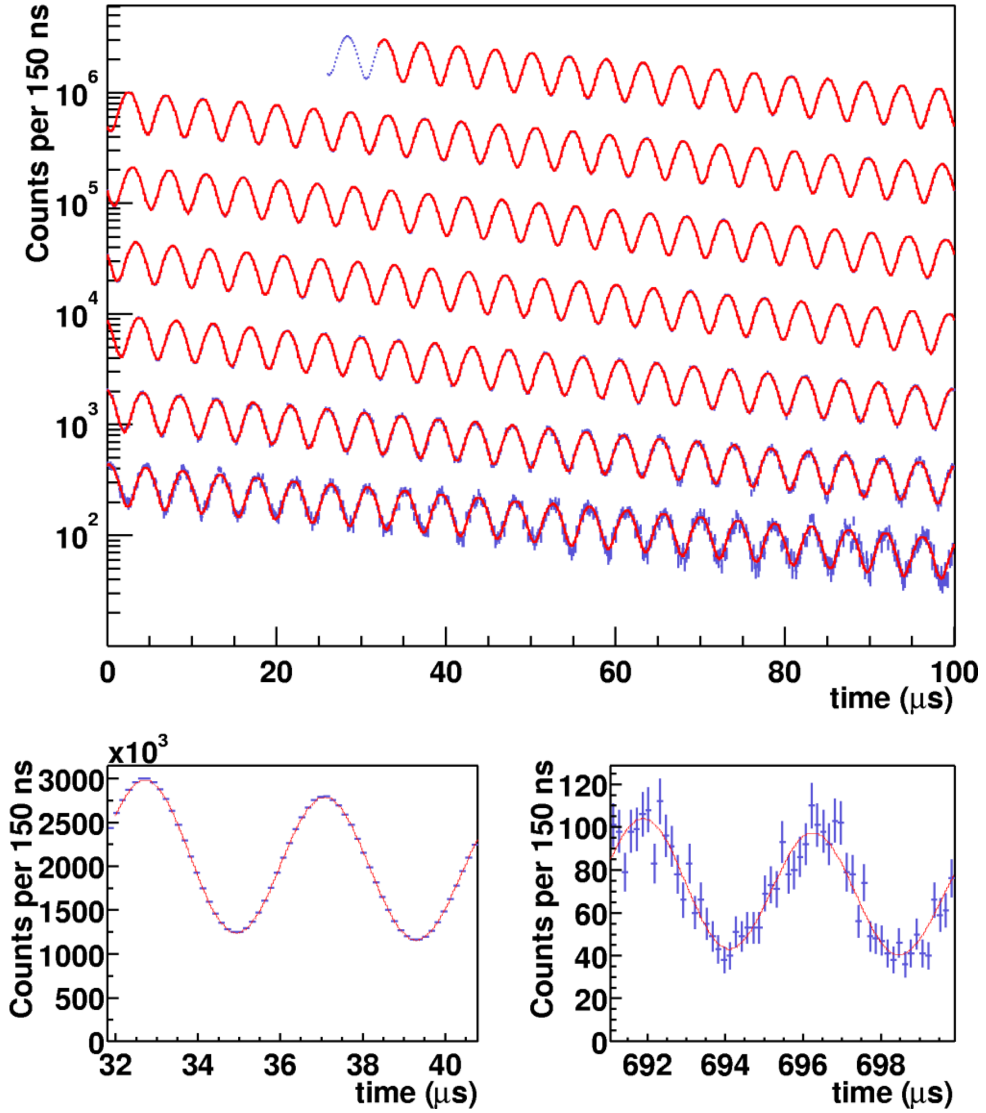

Observed positron rate in successive 100 μs periods
~150 polarisation rotations during measurement period

$$\omega_a \approx \frac{e}{m_\mu c} a_\mu B$$

obtained from time-dependent fit

$$N(t) = N_0 e^{-t/\gamma\tau}[1 - A \cdot \sin(\omega_a t - \phi)]$$

In blue: fit parameters

B field measured with Hall probes with RMN frequency as reference
⇒ a_μ obtained as ratio of 2 frequencies (double blind analysis)

Total systematic uncertainty on ω_a: 0.2–0.3 ppm,
with largest contributors:

- *pileup* (~in-time arrival of two low-*E* electrons)
- *muon losses*
- *coherent betatron* oscillation (muon loss and CBO amplitude [frequency: 0.48 MHz, compared to ω_a: 0.23 MHz] are part of fit)
- *calorimeter gain changes*

$$a_\mu = 11\,659\,209.1\,(5.4)(3.3)\ \cdot 10^{-10}$$

stat syst

Theoretical prediction for a_μ

$$a_\mu^{\text{th}} = a_\mu^{\text{SM}} + a_\mu^{\text{BSM}}$$

$$a_\mu^{\text{SM}} = a_\mu^{\text{QED}} + a_\mu^{\text{had}} + a_\mu^{\text{Weak}}$$

$$a_\mu^{\text{BSM}}$$

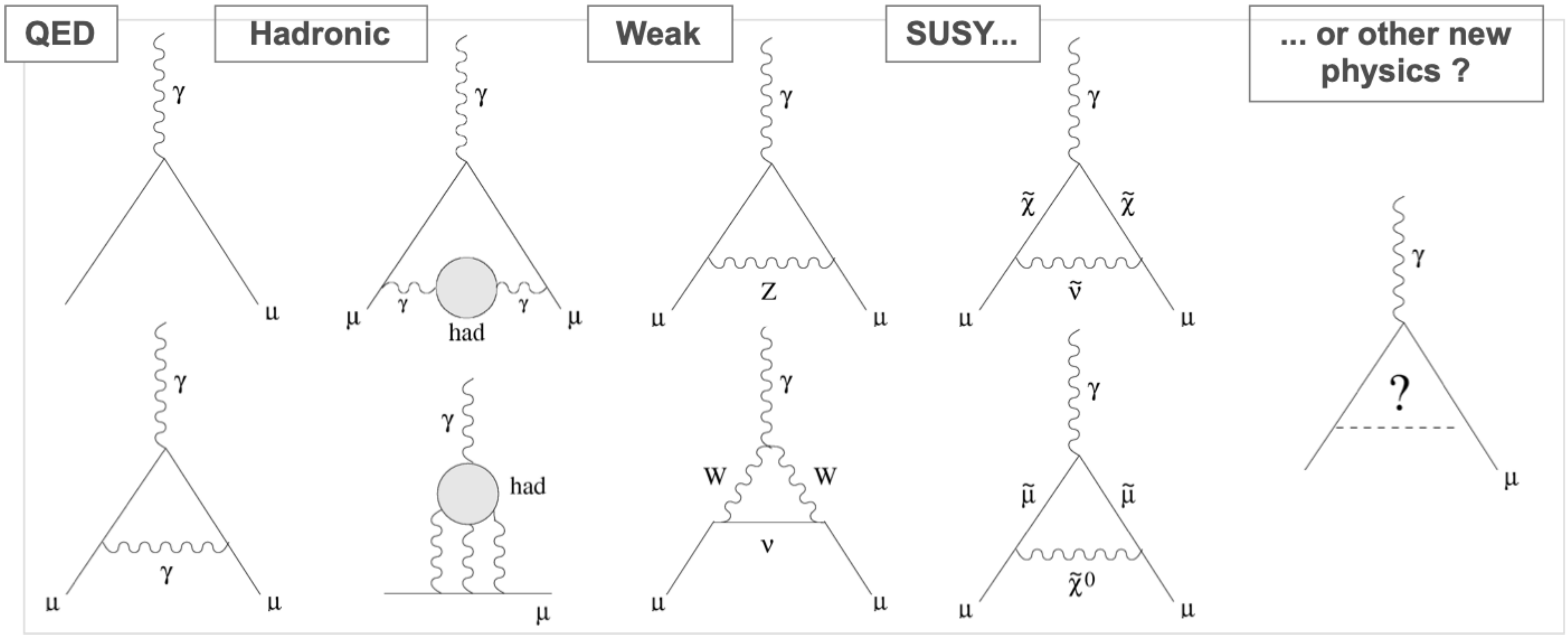

Theoretical prediction for a_μ : QED

Known to 5 loops, good convergence, diagrams with internal electron loops enhanced:

$$a_\mu^{\mathrm{QED}} = \frac{\alpha}{2\pi} + A_2\left(\frac{\alpha}{\pi}\right)^2 + A_3\left(\frac{\alpha}{\pi}\right)^3 + A_4\left(\frac{\alpha}{\pi}\right)^4 + A_5\left(\frac{\alpha}{\pi}\right)^5$$

A_2 A_3 known analytically, A_4 A_5 obtained with Monte Carlo techniques, partially checked analytically for A_4

Aoyama, Hayakawa, Kinoshita, Nio (2012-2019)

α = 137.035 999 046 (27) from Cs recoil measurement (Mueller et al.)

$$\begin{aligned} a_\mu^{\mathrm{QED}} = &\ 116\,140\,973.321\,(23) && \alpha \\ + &\ 413\,217.626\ \ (7) && \alpha^2 \\ + &\ 30\,141.902\,(33) \quad (\times 10^{-11}) && \alpha^3 \\ + &\ 381.004\,(17) && \alpha^4 \\ + &\ 5.078\ \ (6) && \alpha^5 \\ = &\ 116\,584\,718.931\,(104) \end{aligned}$$

12672 diagrams

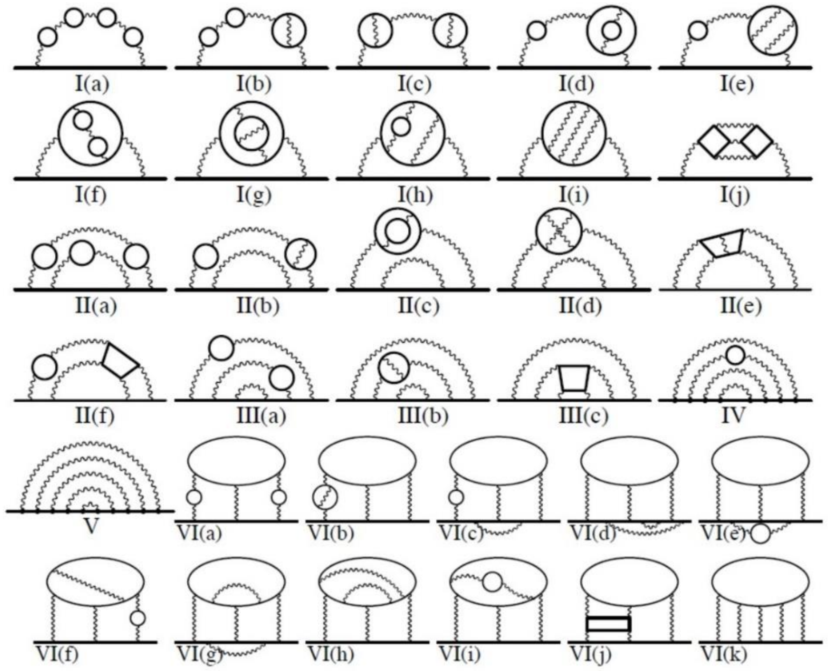

uncertainty dominated by estimate on α^6 term

Theoretical prediction for a_μ : EW, hadronic light-by-light

- EW: one-loop + two-loop involving W, Z bosons (little sensitivity to Higgs boson mass)

$$a_\mu^{EW} = 153.6\ (1.0) \times 10^{-11}$$

shows level of sensitivity of a_μ to physics at large mass scales ~ O(0.1 TeV)

Precision at low energies ⇔ high energy frontier

- Hadronic light-by-light: α^3 contribution not computable by analytical QCD; so far only estimated by phenomenological models using intermediate particles; new approach partly using experimental data (2017); also first results from QCD lattice simulations (2019)

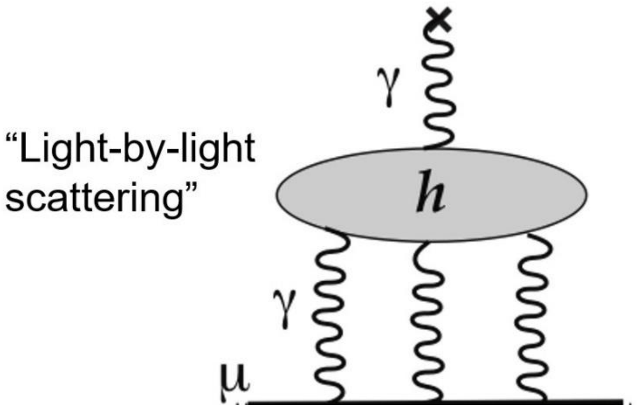

small contribution

$$a_\mu^{HLbL} = 94\ (19) \times 10^{-11}$$

Theoretical prediction for a_μ : Hadronic Vacuum Polarization

Dominant uncertainty for the theoretical prediction from HVP part which cannot be calculated from QCD (low mass scale), but one can use experimental data on $e^+ e^- \rightarrow$ hadrons cross section

Born: $\sigma^{(0)}(s) = \sigma(s)\left(\alpha / \alpha(s)\right)^2$

$$12\pi \, \mathrm{Im}\Pi_\gamma(s) = \frac{\sigma^0 \left[e^+e^- \rightarrow \mathrm{hadrons}\,(\gamma_{FSR})\right]}{\sigma_{pt}} \equiv R(s)$$

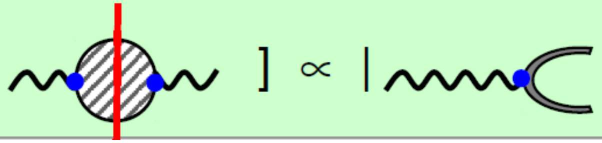

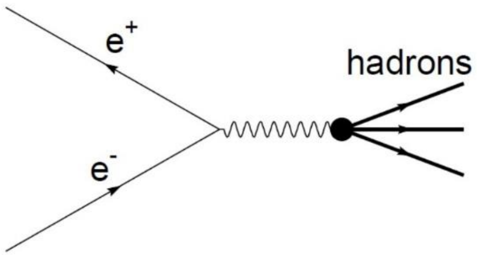

- unitarity
- analyticity

⇒ dispersion relation

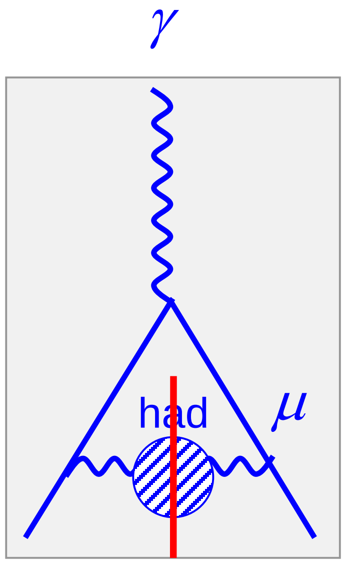

$$a_\mu^{\mathrm{had}} = \frac{\alpha^2}{3\pi^2} \int_{4m_\pi^2}^{\infty} ds \, \frac{K(s)}{s} R(s)$$

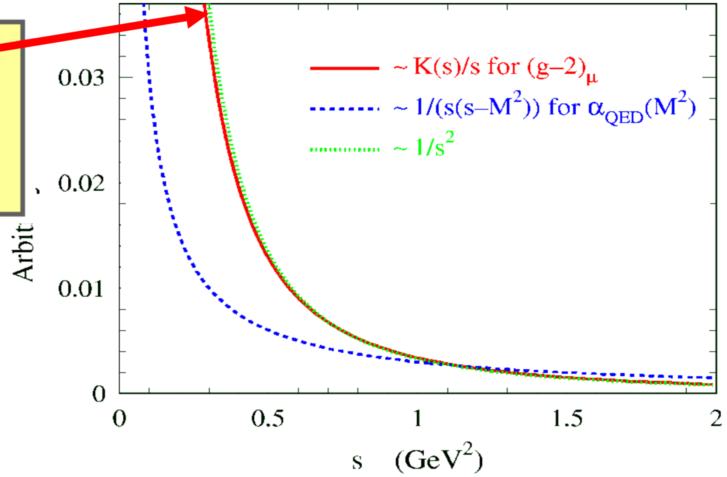

Bouchiat-Michel (1961)
Brodsky-de Rafael (1968)

Precise $\sigma(e^+e^- \rightarrow \mathrm{hadrons})$ measurements at low energy are necessary

Hadronic Vacuum Polarization (DHMZ group)

- HVP has been for long and still now the largest contribution to the uncertainty of the a_μ prediction in the SM
- Limited by the accuracy of e+e- experimental data
- DHMZ group (MD, Andreas Hoecker, Bogdan Malaescu, Zhiqing Zhang) involved since 1997
- Result used as reference for the Brookhaven experiment: comparison revealed a deficit in the prediction at ~ 2-3 σ level, hence our motivation to continue this effort toward a more precise prediction

- Main contributions to data treatment
  - Compilation of existing data for e+e- annihilation to obtain R as a sum of exclusive processes
  - Robust combination techniques taking into account all correlated uncertainties as function of energy, between exclusive channels, and between experiments
  - Correct for unmeasured processes using isospin constraints
  - Determine energy regions where perturbative QCD calculations are safe (experience with τ physics at LEP)

- Launched a dedicated program of e+e- cross section measurements using the BABAR detector (Stanford) to get more precise data (2001-2014) with the new Initial State Radiation (ISR) method. A new phase is still underway.

- Same data and techniques used to study the running of α (energy) from $\alpha(0)$ to $\alpha(M_Z)$ $\Rightarrow$ prediction for M_{Higgs}

- Double role as phenomenologists and experimenters

Measurements of $\sigma(e^+e^- \to \text{hadrons})$

1. The scan method: e.g. CMD-2/3, SND at Novosibirsk
   - ➢ Advantages:
     - ➢ Well defined √s
     - ➢ Good energy resolution ~10^{-3}√s
   - ➢ Disadvantages:
     - ➢ Energy gap between two scans
     - ➢ Low luminosity at low energies
     - ➢ Limited √s range of a given experiment

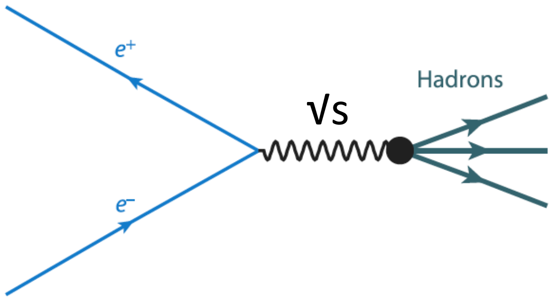

2. The ISR approach: e.g. BaBar, KLOE, BES, CLEOc
   - ➢ Advantages:
     - ➢ Continuous cross section measurement over a broad energy range down to threshold
     - ➢ large acceptance for hadrons if ISR detected at large angle
     - ➢ $\sigma(e^+e^- \to \text{hadrons})$ may be measured over $\sigma(e^+e^- \to \mu^+\mu^-)$ thus reducing some syst uncertainties
   - ➢ Disadvantages:
     - ➢ Requires high luminosity to compensate higher order in α

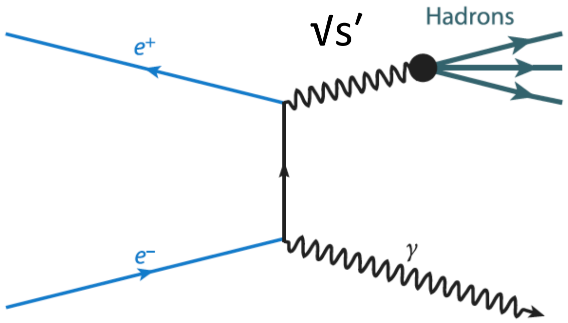

$s' = (1-x)/s$
$x = 2E_\gamma/\sqrt{s}$

Combining cross section data (HVPTools)

- Combine experimental spectra with arbitrary point spacing / binning
- Properly propagate uncertainties and correlations

  - *Between measurements (data points/bins) of a given experiment* (covariance matrices and/or detailed split of uncertainties)
  - *Between experiments* (common systematic uncertainties, e.g. VP)
  - *Between different channels*, e.g. luminosity, radiative corrections, some efficiencies

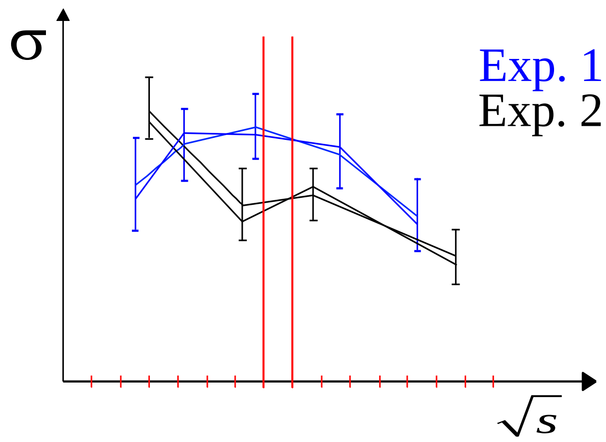

- Linear/quadratic splines to interpolate between the points/bins of each experiment
- Fluctuate data points taking into account correlations and re-do the splines for each (pseudo-)experiment
  - each uncertainty fluctuated coherently for all the points/bins that it impacts
  - eigenvector decomposition for (statistical & systematic) covariance matrices
- Integral(s) evaluated for nominal result and for each set of toy pseudo-experiments; uncertainty of integrals from RMS of results for all toys
- Pseudo-experiments also used to derive (statistical & systematic) covariance matrices of combined cross sections

  → Integral evaluation

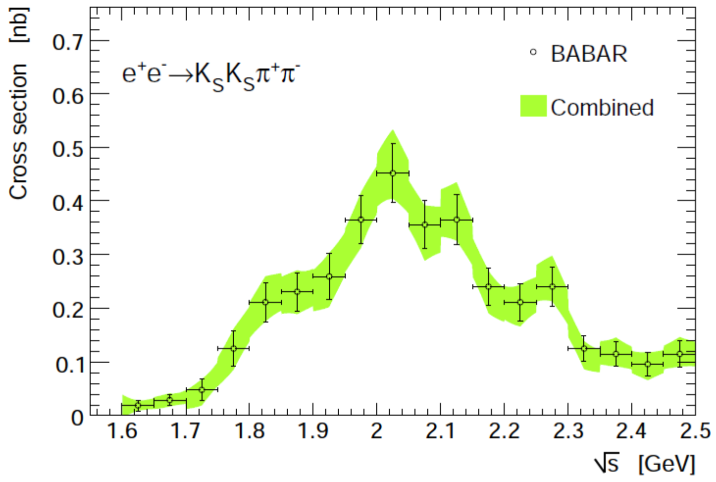

Different energy regions for R(s)

Davier-Hoecker-Zhang, RMP 78 (2006) 1043

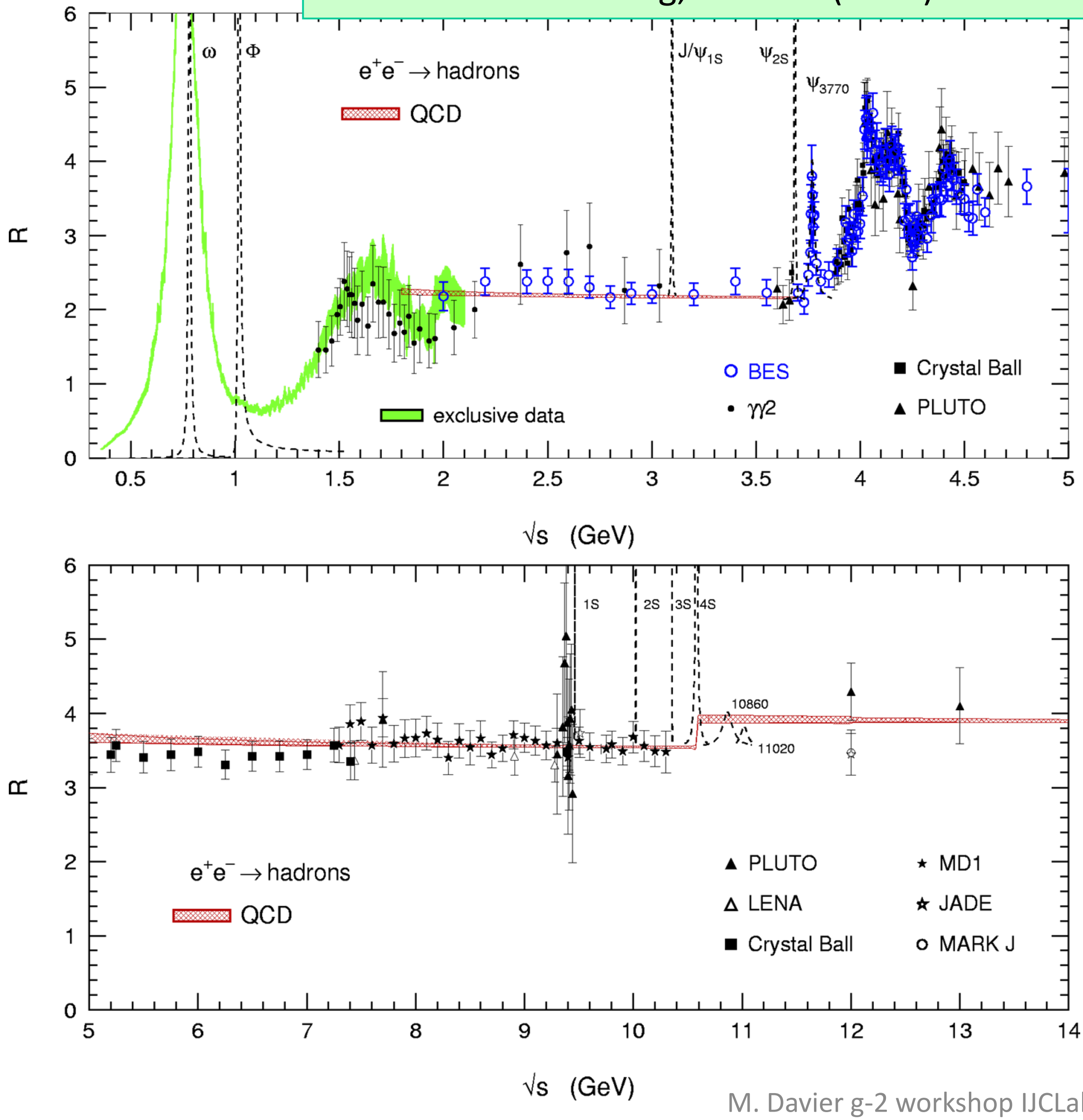

- [$\pi^0\gamma$ threshold-1.8GeV]
  - sum about 22→37 exclusive channels
  - estimate unmeasured channels using isospin relations (now < 0.1%)
- [1.8-3.7] GeV
  - good agreement between data and pQCD calculation → use 4-loop pQCD
  - J/ψ, ψ(2s): Breit-Wigner integral
- [3.7-5] GeV
  use data
- >5GeV
  use 4-loop pQCD calculation

The dominant channel : $e^+e^- \to \pi^+ \pi^-(\gamma)$

73% of HVP contribution to a_μ

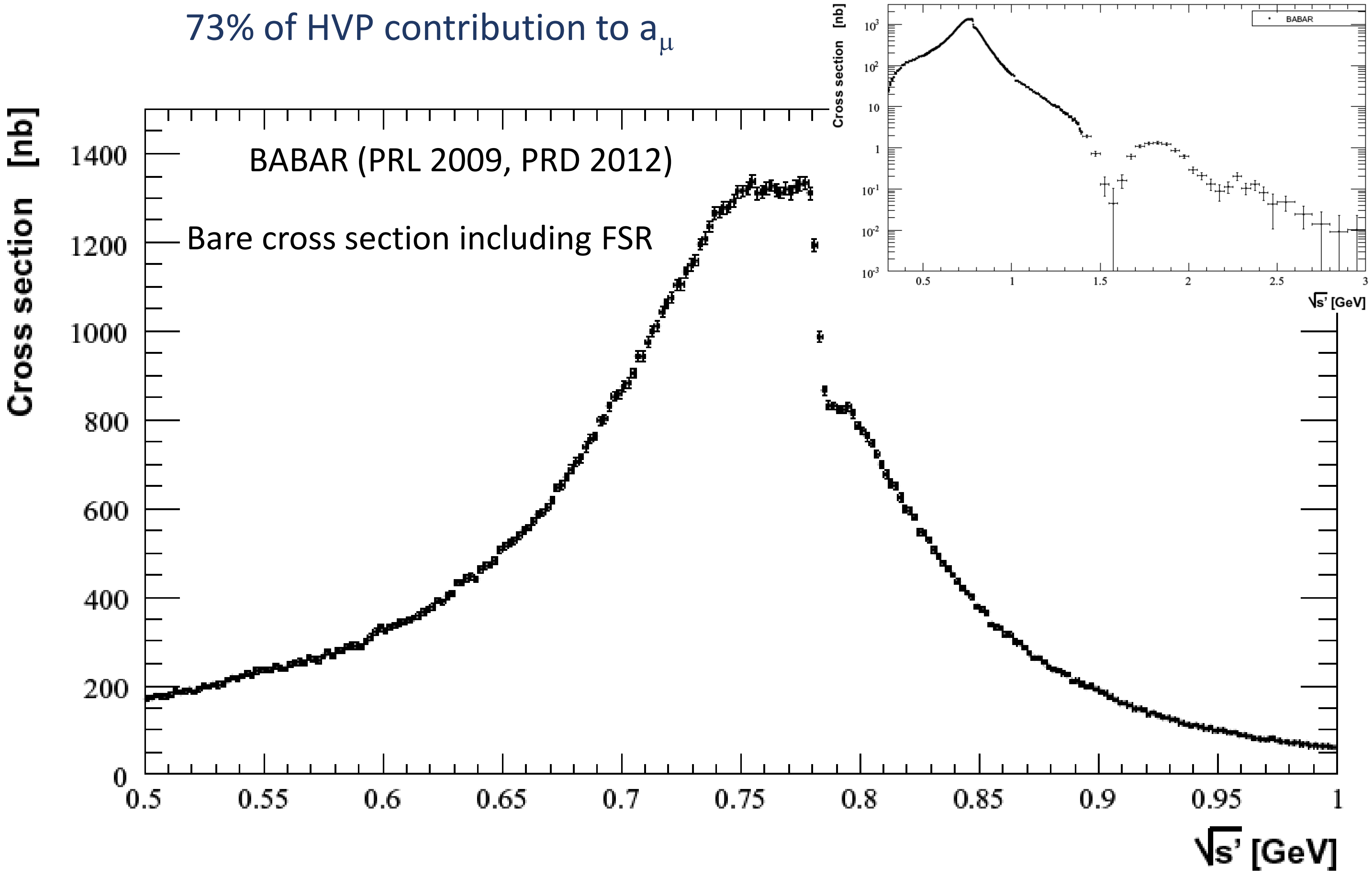

BABAR: multi-hadronic channels

Besides our team for the leading $\pi^+\pi^-$ and K^+K^- cross sections, other BABAR groups have taken the lead to measure the rest of exclusive cross sections (altogether ~ 40 processes)

$\Rightarrow$ complete and precise reconstruction of R below 2 GeV

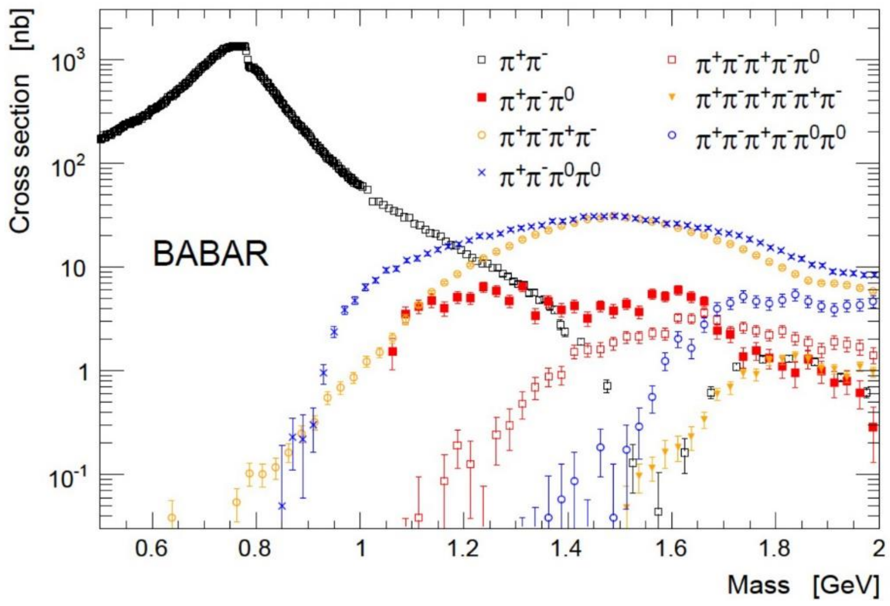

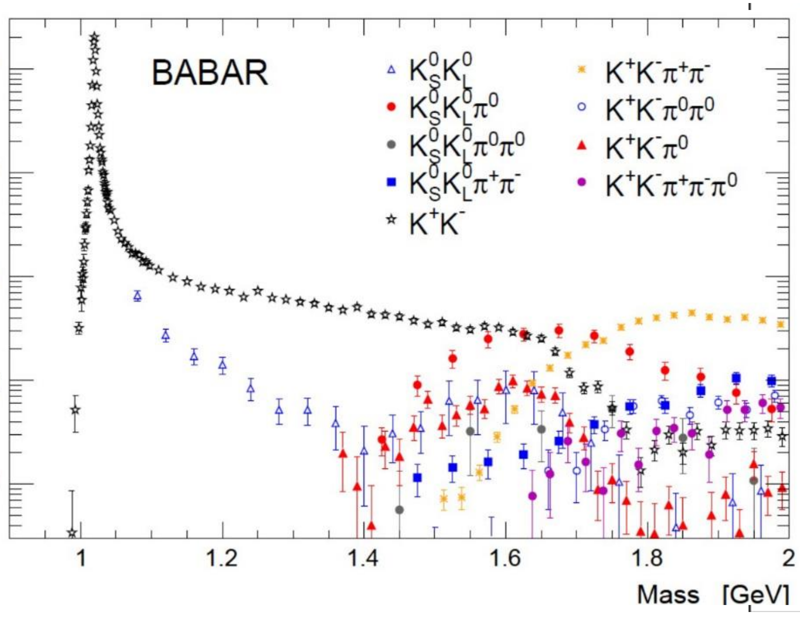

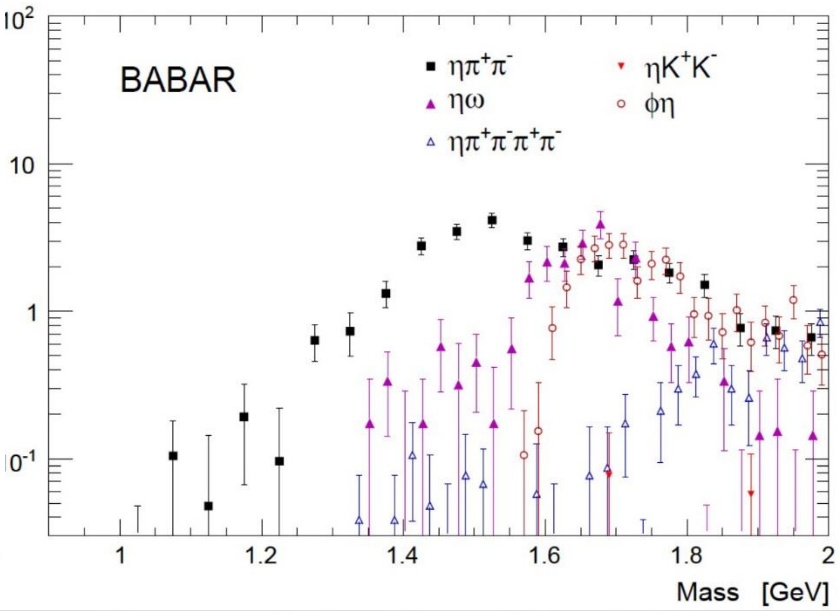

Combination : $e^+e^- \to \pi^+\pi^-(\gamma)$

Figures from DHMZ, EPJC80 (2020) 241

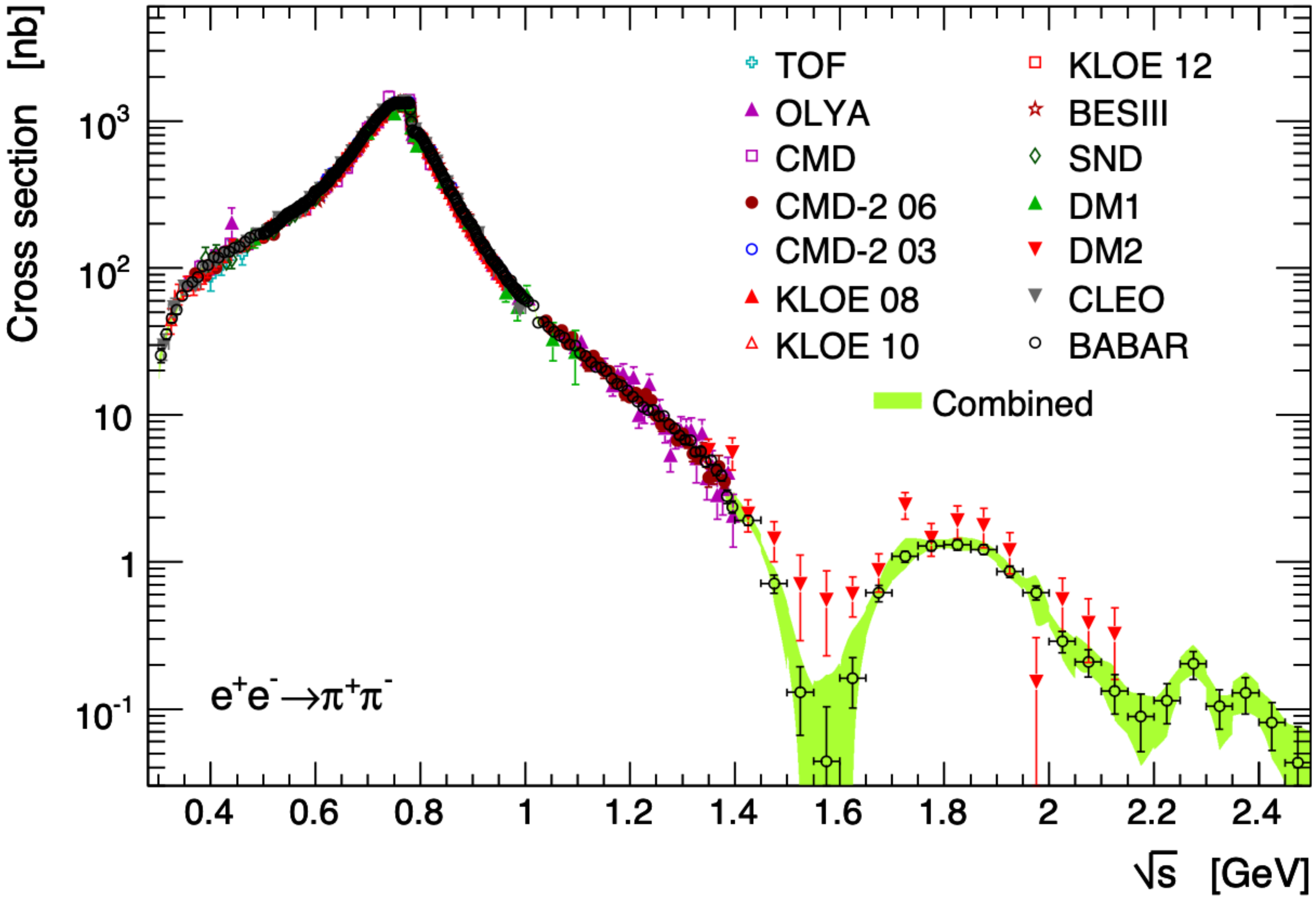

Consistency between experimental data

- Latest dispersive evaluations rely on a rather complete set of measurements of $e^+e^- \to$ hadrons up to 6π, $\eta 4\pi$, $KK2\pi$ in all charge configurations, and a few more higher-multiplicity processes
- missing channels in the range [1.5-1.8] GeV are estimated to contribute < 0.1% using isospin symmetry
- discrepancies exist in the K^+K^- channel on the $\varphi(1020)$ (CMD-3 vs. CMD-2, SND, BABAR), taken into account
- A more significant discrepancy occurs in the $\pi^+\pi^-$ channel between the 2 most precise results (BABAR and KLOE)
- Taking into account the BABAR/KLOE disagreement in the combination, all experiments are in agreement within an enlarged combination uncertainty (0.7%), already a remarkable result given different experimental conditions: ISR (10.6 GeV BABAR, ~4 GeV BES CLEOc, 1.02 GeV KLOE), direct scan (CMD-2, SND)

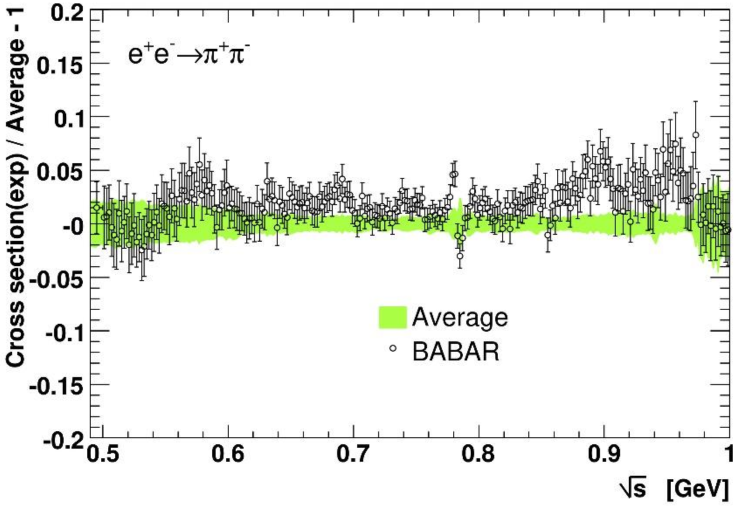

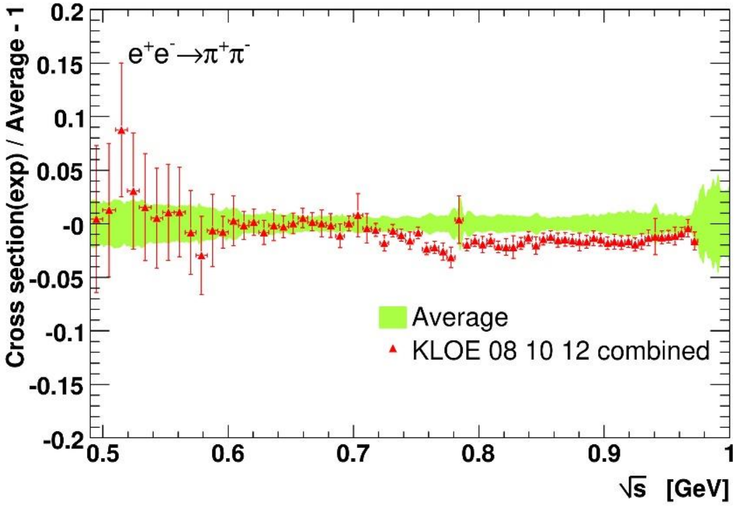

Figure from DHMZ, EPJC80 (2020) 241

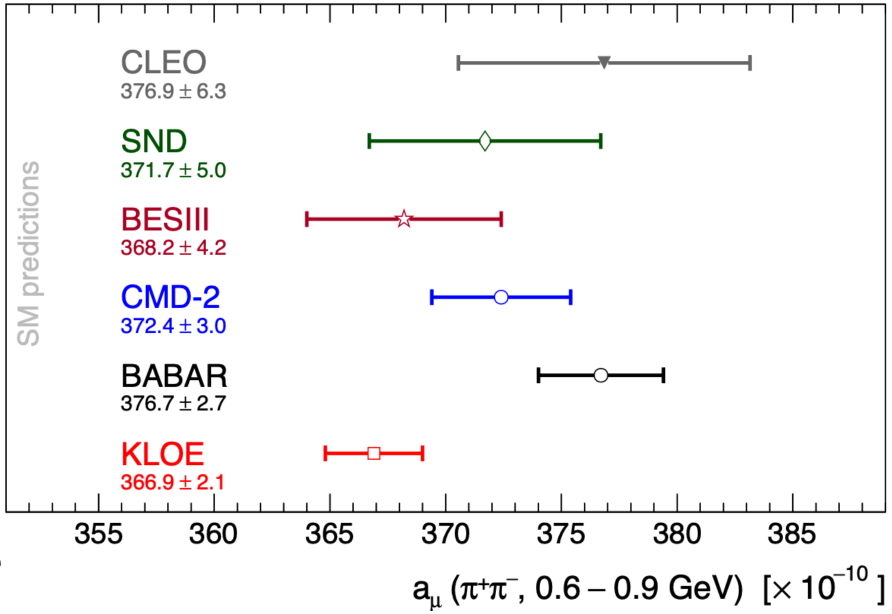

- Additional systematic error added because of BABAR-KLOE difference $\Rightarrow$ degrades uncertainty by 30%

The current R(s) (DHMZ19)

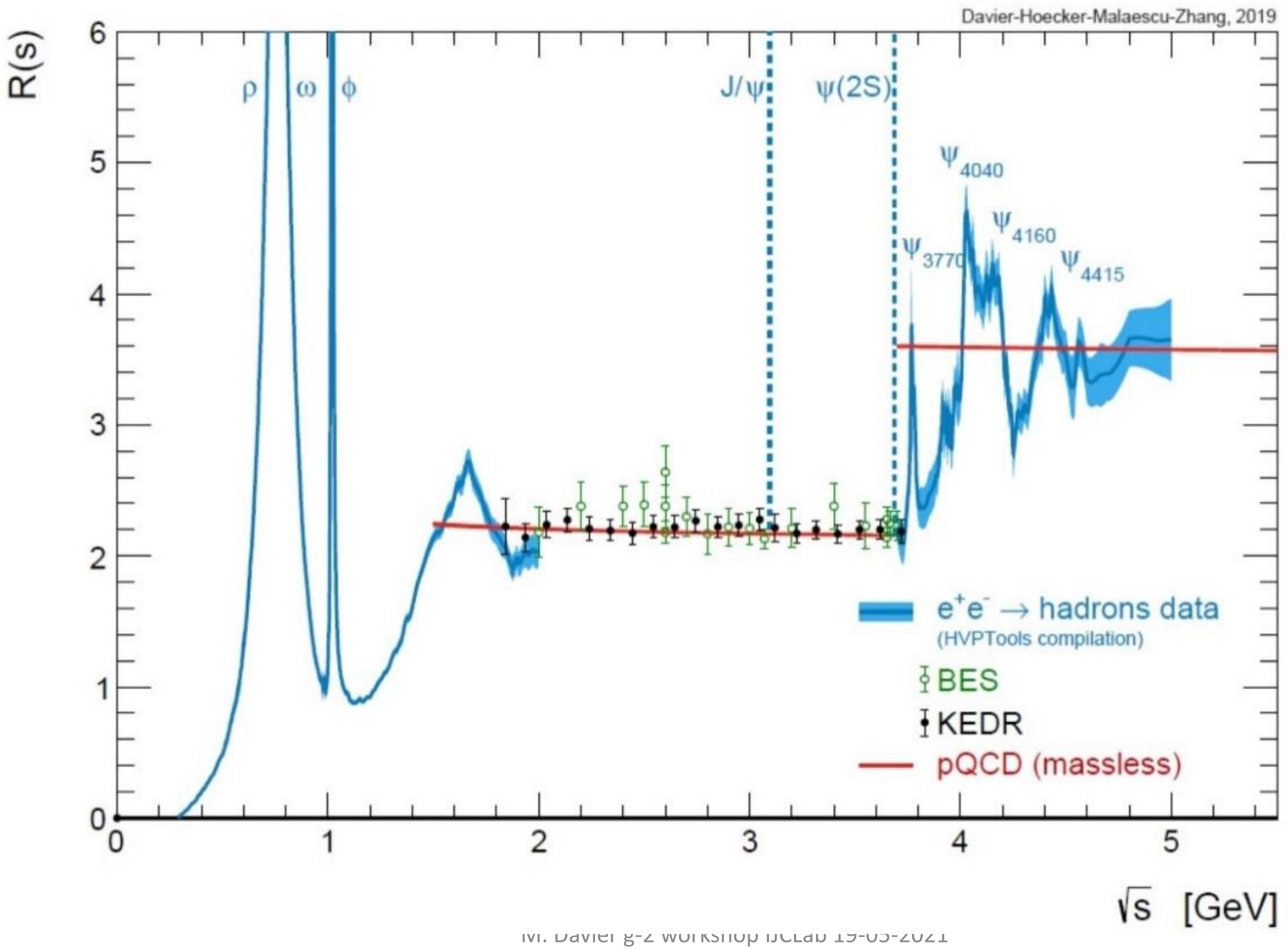

All contributions (DHMZ19)

Channel	$a_\mu^{\text{had, LO}}[10^{-10}]$	$\Delta\alpha(m_Z^2)[10^{-4}]$
$\pi^0\gamma$	$4.29 \pm 0.06 \pm 0.04 \pm 0.07$	$0.35 \pm 0.00 \pm 0.00 \pm 0.01$
$\eta\gamma$	$0.65 \pm 0.02 \pm 0.01 \pm 0.01$	$0.08 \pm 0.00 \pm 0.00 \pm 0.00$
$\pi^+\pi^-$	$507.80 \pm 0.83 \pm 3.19 \pm 0.60$	$34.49 \pm 0.06 \pm 0.20 \pm 0.04$
$\pi^+\pi^-\pi^0$	$46.20 \pm 0.40 \pm 1.10 \pm 0.86$	$4.60 \pm 0.04 \pm 0.11 \pm 0.08$
$2\pi^+2\pi^-$	$13.68 \pm 0.03 \pm 0.27 \pm 0.14$	$3.58 \pm 0.01 \pm 0.07 \pm 0.03$
$\pi^+\pi^-2\pi^0$	$18.03 \pm 0.06 \pm 0.48 \pm 0.26$	$4.45 \pm 0.02 \pm 0.12 \pm 0.07$
$2\pi^+2\pi^-\pi^0$ (η excl.)	$0.69 \pm 0.04 \pm 0.06 \pm 0.03$	$0.21 \pm 0.01 \pm 0.02 \pm 0.01$
$\pi^+\pi^-3\pi^0$ (η excl.)	$0.49 \pm 0.03 \pm 0.09 \pm 0.00$	$0.15 \pm 0.01 \pm 0.03 \pm 0.00$
$3\pi^+3\pi^-$	$0.11 \pm 0.00 \pm 0.01 \pm 0.00$	$0.04 \pm 0.00 \pm 0.00 \pm 0.00$
$2\pi^+2\pi^-2\pi^0$ (η excl.)	$0.71 \pm 0.06 \pm 0.07 \pm 0.14$	$0.25 \pm 0.02 \pm 0.02 \pm 0.05$
$\pi^+\pi^-4\pi^0$ (η excl., isospin)	$0.08 \pm 0.01 \pm 0.08 \pm 0.00$	$0.03 \pm 0.00 \pm 0.03 \pm 0.00$
$\eta\pi^+\pi^-$	$1.19 \pm 0.02 \pm 0.04 \pm 0.02$	$0.35 \pm 0.01 \pm 0.01 \pm 0.01$
$\eta\omega$	$0.35 \pm 0.01 \pm 0.02 \pm 0.01$	$0.11 \pm 0.00 \pm 0.01 \pm 0.00$
$\eta\pi^+\pi^-\pi^0(\text{non-}\omega, \phi)$	$0.34 \pm 0.03 \pm 0.03 \pm 0.04$	$0.12 \pm 0.01 \pm 0.01 \pm 0.01$
$\eta 2\pi^+2\pi^-$	$0.02 \pm 0.01 \pm 0.00 \pm 0.00$	$0.01 \pm 0.00 \pm 0.00 \pm 0.00$
$\omega\eta\pi^0$	$0.06 \pm 0.01 \pm 0.01 \pm 0.00$	$0.02 \pm 0.00 \pm 0.00 \pm 0.00$
$\omega\pi^0$ ($\omega \to \pi^0\gamma$)	$0.94 \pm 0.01 \pm 0.03 \pm 0.00$	$0.20 \pm 0.00 \pm 0.01 \pm 0.00$
$\omega(\pi\pi)^0$ ($\omega \to \pi^0\gamma$)	$0.07 \pm 0.00 \pm 0.00 \pm 0.00$	$0.02 \pm 0.00 \pm 0.00 \pm 0.00$
ω (non-$3\pi, \pi\gamma, \eta\gamma$)	$0.04 \pm 0.00 \pm 0.00 \pm 0.00$	$0.00 \pm 0.00 \pm 0.00 \pm 0.00$
K^+K^-	$23.08 \pm 0.20 \pm 0.33 \pm 0.21$	$3.35 \pm 0.03 \pm 0.05 \pm 0.03$
K_SK_L	$12.82 \pm 0.06 \pm 0.18 \pm 0.15$	$1.74 \pm 0.01 \pm 0.03 \pm 0.02$
ϕ (non-$K\overline{K}, 3\pi, \pi\gamma, \eta\gamma$)	$0.05 \pm 0.00 \pm 0.00 \pm 0.00$	$0.01 \pm 0.00 \pm 0.00 \pm 0.00$
$K\overline{K}\pi$	$2.45 \pm 0.05 \pm 0.10 \pm 0.06$	$0.78 \pm 0.02 \pm 0.03 \pm 0.02$
$K\overline{K}2\pi$	$0.85 \pm 0.02 \pm 0.05 \pm 0.01$	$0.30 \pm 0.01 \pm 0.02 \pm 0.00$
$K\overline{K}3\pi$ (estimate)	$-0.02 \pm 0.01 \pm 0.01 \pm 0.00$	$-0.01 \pm 0.00 \pm 0.00 \pm 0.00$
$\eta\phi$	$0.33 \pm 0.01 \pm 0.01 \pm 0.00$	$0.11 \pm 0.00 \pm 0.00 \pm 0.00$
$\eta K\overline{K}$ (non-ϕ)	$0.01 \pm 0.01 \pm 0.01 \pm 0.00$	$0.00 \pm 0.00 \pm 0.01 \pm 0.00$
$\omega K\overline{K}$ ($\omega \to \pi^0\gamma$)	$0.01 \pm 0.00 \pm 0.00 \pm 0.00$	$0.00 \pm 0.00 \pm 0.00 \pm 0.00$
$\omega 3\pi$ ($\omega \to \pi^0\gamma$)	$0.06 \pm 0.01 \pm 0.01 \pm 0.01$	$0.02 \pm 0.00 \pm 0.00 \pm 0.00$
7π ($3\pi^+3\pi^-\pi^0$ + estimate)	$0.02 \pm 0.00 \pm 0.01 \pm 0.00$	$0.01 \pm 0.00 \pm 0.00 \pm 0.00$
J/ψ (BW integral)	6.28 ± 0.07	7.09 ± 0.08
$\psi(2S)$ (BW integral)	1.57 ± 0.03	2.50 ± 0.04
R data [3.7 − 5.0] GeV	$7.29 \pm 0.05 \pm 0.30 \pm 0.00$	$15.79 \pm 0.12 \pm 0.66 \pm 0.00$
R_{QCD} $[1.8 - 3.7\ \text{GeV}]_{uds}$	$33.45 \pm 0.28 \pm 0.65_{\text{dual}}$	$24.27 \pm 0.18 \pm 0.28_{\text{dual}}$
R_{QCD} $[5.0 - 9.3\ \text{GeV}]_{udsc}$	6.86 ± 0.04	34.89 ± 0.17
R_{QCD} $[9.3 - 12.0\ \text{GeV}]_{udscb}$	1.21 ± 0.01	15.56 ± 0.04
R_{QCD} $[12.0 - 40.0\ \text{GeV}]_{udscb}$	1.64 ± 0.00	77.94 ± 0.12
R_{QCD} $[> 40.0\ \text{GeV}]_{udscb}$	0.16 ± 0.00	42.70 ± 0.06
R_{QCD} $[> 40.0\ \text{GeV}]_{t}$	0.00 ± 0.00	-0.72 ± 0.01
Sum	$693.9 \pm 1.0 \pm 3.4 \pm 1.6 \pm 0.1_\psi \pm 0.7_{\text{QCD}}$	$275.42 \pm 0.15 \pm 0.72 \pm 0.23 \pm 0.09_\psi \pm 0.55_{\text{QCD}}$

40 exclusive channels (<1.8 GeV) evaluated

Estimation for missing modes based on isospin constraints becomes negligible (0.016%)

Table taken from DHMZ, EPJC80 (2020) 241

The g-2 theory initiative (2017-2020)

- By 2012, prediction using more precise e+e- data confirmed the discrepancy with the Brookhaven measurement, reaching ~ 3.5 σ

- In view of forthcoming results from the new g-2 direct experiment at Fermilab, a concerted effort was organized to try to produce the most reliable prediction ahead of time (blind to the new result)

- Organized 6 workshops followed by ~ 130 physicists (many lattice QCD theorists)

- Progress in hadronic LbL calculations with phenomenological and lattice methods, uncertainty reduced

- For HVP
  - ➢ lattice groups very active, but could not produce a reliable and competitive result
  - ➢ the dispersive approach based on data was adopted: results of 2 groups used (DHMZ and KNT) with the DHMZ conservative approach of estimating uncertainties prevailing

- Comprehensive report (166 pages) ready early 2020 and published in Physics Reports, well before the Fermilab release

The g-2 theory initiative prediction (WP2020)

HVP

HLbL

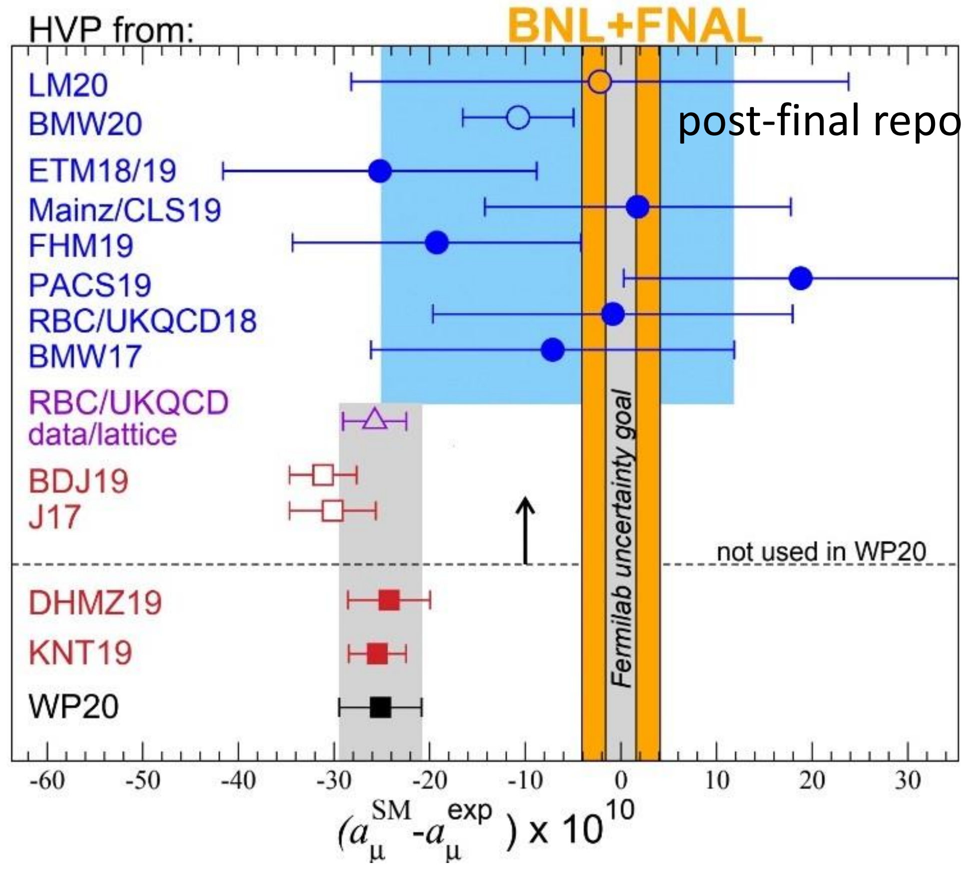

post-final report (see later)

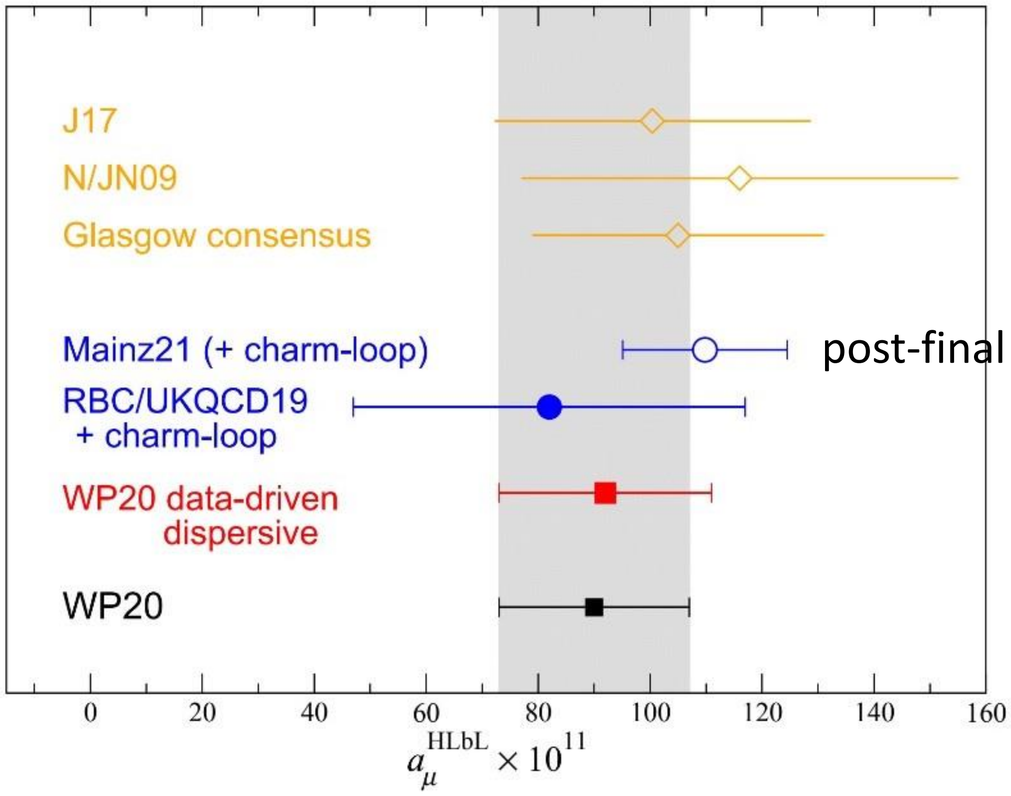

post-final report

The muon g-2 Fermilab experiment

- Brookhaven experiment limited by statistics, systematic effects well understood, could be improved with more intense (x 20) and pure muon beam at Fermilab
- Goal: reduce final uncertainty by a factor of 4 (over several years)
- Enlarged collaboration
- Experiment completely redesigned (beam instrumentation, detectors, electronics), only superconducting magnet kept and shipped

The muon g-2 Fermilab experiment: a few features

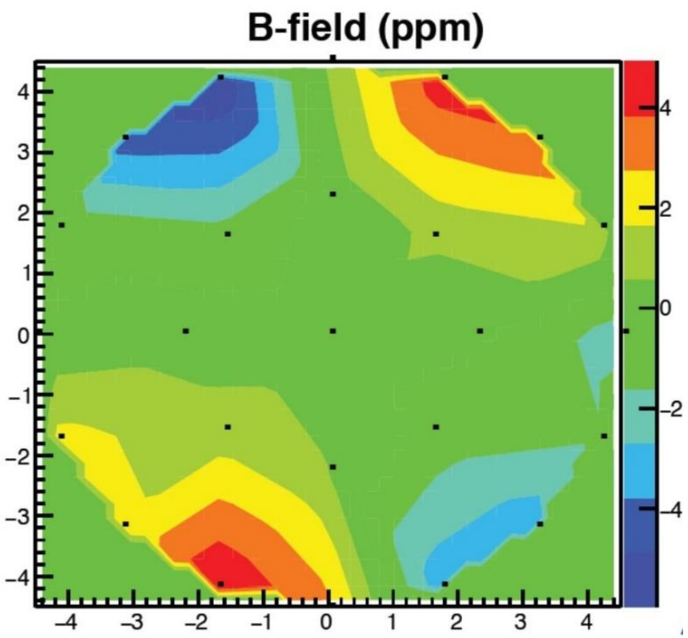

- B-field uniformity after careful magnet shimming
- Checked every 3 days with special trolley with probes
- Large number of fixed probes to interpolate shifts
- Real-time reconstruction of muon beam position/shape to obtain B-field as seen by the muons
- Possible using tracking system of electron detectors
- Calorimeters with PbF2 crystals read-out by SiPM's (reduce pile-up)

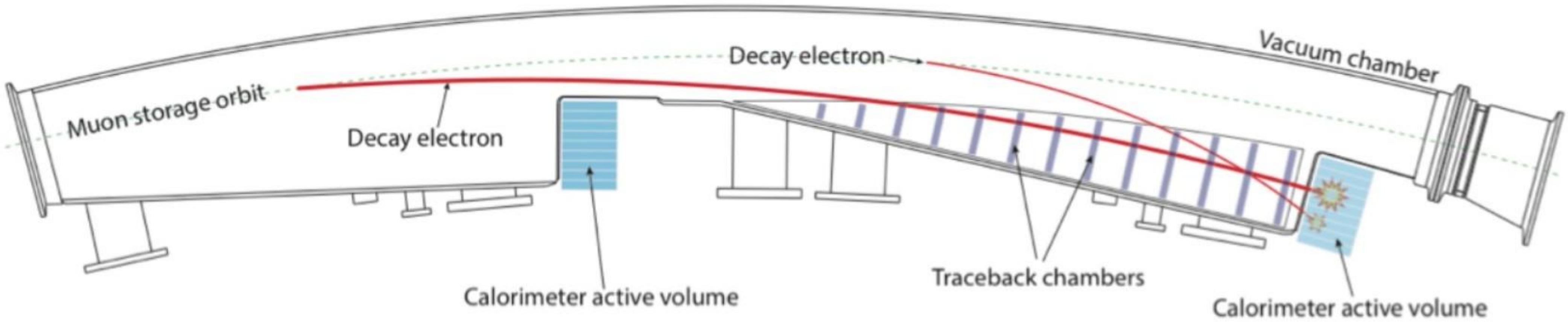

The muon g-2 Fermilab experiment: correcting systematic effects

- Large number of systematic studies to establish corrections and to estimate uncertainties
- Beam distortions/oscillations
- Muon losses
- E-field residual effect
- Different methods for ω_a determination
- B-field (ω_p)
- Several groups for each topics
- Double unblinding for ω_a and ω_p with secret offsets for clock frequencies

- precision dominated by statistics
- Guarantees progress for future analyses (so far only 6% of total data)

Quantity	Correction Terms (ppb)	Uncertainty (ppb)
ω_a (statistical)	–	434
ω_a (systematic)	–	56
C_e	489	53
C_p	180	13
C_{ml}	-11	5
C_{pa}	-158	75
$f_{calib}\langle\omega_p'(x,y,\phi) \times M(x,y,\phi)\rangle$	–	56
B_q	-17	92
B_k	-27	37
$\mu_p'(34.7°)/\mu_e$	–	10
m_μ/m_e	–	22
$g_e/2$	–	0
Total	–	462

434 ppb stat $\oplus$ 157 ppb syst error

The muon g-2 Fermilab experiment: the result

$$a_\mu(\text{Fermilab}) = 116\,592\,040\,(54) \times 10^{-11}$$

- Agreement with Brookhaven value
- Precision comparable

- Excess / SM prediction increased to 4.2σ

- Caution about significance:
  - ➢ statistics-dominated measurement
  - ➢ prediction uncertainty limited by systematic effects (not Gaussian)

- Nevertheless, large discrepancy (the largest so far between measurement and SM anywhere)

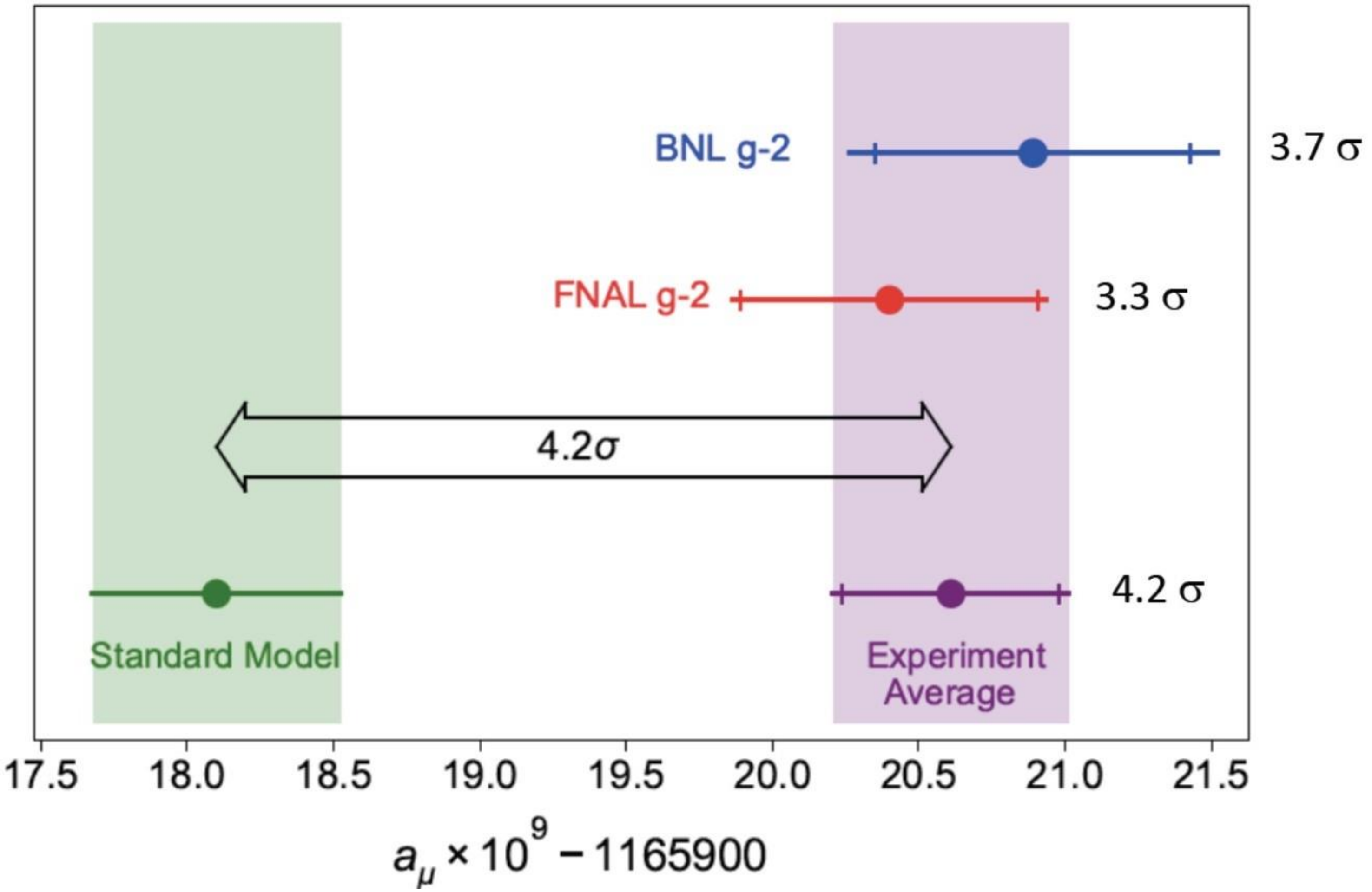

60 years of muon g-2 measurements and theory predictions

Experiment	Beam	Measurement	$\delta a_\mu / a_\mu$	Required th. terms
Columbia-Nevis (57)	μ^+	g=2.00±0.10		g=2
Columbia-Nevis (59)	μ^+	0.001 13(+16)(−12)	12.4%	α/π
CERN 1 (61)	μ^+	0.001 145(22)	1.9%	α/π
CERN 1 (62)	μ^+	0.001 162(5)	0.43%	$(\alpha/\pi)^2$
CERN 2 (68)	μ^+	0.001 166 16(31)	265 ppm	$(\alpha/\pi)^3$
CERN 3 (75)	$\mu^\pm$	0.001 165 895(27)	23 ppm	$(\alpha/\pi)^3$ + had
CERN 3 (79)	$\mu^\pm$	0.001 165 911(11)	7.3 ppm	$(\alpha/\pi)^3$ + had
BNL E821 (00)	μ^+	0.001 165 919 1(59)	5 ppm	$(\alpha/\pi)^3$ + had
BNL E821 (01)	μ^+	0.001 165 920 2(16)	1.3 ppm	$(\alpha/\pi)^4$ + had + weak
BNL E821 (02)	μ^+	0.001 165 920 3(8)	0.7 ppm	$(\alpha/\pi)^4$ + had + weak + ?
BNL E821 (04)	μ^-	0.001 165 921 4(8)(3)	0.7 ppm	$(\alpha/\pi)^4$ + had + weak + ?
New → FNAL Run1 (21)	μ^+	0.001 165 920 40(54)	0.46 ppm	$(\alpha/\pi)^4$ + had + weak + ? (?)

Summary and perspectives

- New measurement of the muon magnetic anomaly released at Fermilab
- Result in agreement with previous Brookhaven experiment
- A large effort was devoted to produce a reliable and conservative theoretical prediction within the Standard Model
- The Hadronic Vacuum Polarization contribution plays a very important role in the value and accuracy of the prediction
- The DHMZ group at Orsay has more than 20 years of experience using the mature dispersive approach based on experimental data on e+e- cross sections and in providing precise data with innovative methods
- Presently the confrontation theory/experiment indicates a missing contribution in the Standard Model at more than 4 σ
- Prospects for improving the direct measurement at Fermilab look good (reduction of uncertainty by a factor of 4 over the next 4 years)
- A new experiment is under preparation at JPARC in Japan using a completely different approach, thus allowing to crosscheck the traditional method

Backup slides

List of DHMZ publications

1. ADH 1998, Eur.Phys.J.C 2 (1998) 123 [330 citations*]
2. DH 1998, Phys.Lett.B 419 (1998) 419 [219 citations]
3. DH 1998, Phys.Lett.B 435 (1998) 427 [292 citations]
4. DEHZ 2003, Eur.Phys.J.C 27 (2003) 497 [394 citations]
5. DEHZ 2003, Eur.Phys.J.C 31 (2003) 503 [430 citations]
6. DHMZ+ 2010, Eur.Phys.J.C 66 (2010) 127 [157 citations]
7. DHMYZ 2010, Eur.Phys.J.C 66 (2010) 1 [209 citations]
8. DHMZ 2011, Eur.Phys.J.C 71 (2011) 1515 [866 citations]
9. DHMZ 2017, Eur.Phys.J.C 77 (2017) 827 [259 citations]
10. DHMZ 2019, Eur.Phys.J.C 80 (2020) 241 [169 citations]
11. Theory initiative WP 2020, Phys.Rept. 887 (2020) 1 [171 citations]

→Total number of citations: ~3500

* Status of April 9, 2021

The ISR method at BABAR

BABAR, operating on the high-luminosity asymmetric PEP II e+e- collider, was designed to study CP violation in the B-antiB system and led to the validation of the Cabibbo-Kobayashi-Maskawa matrix. The ISR program was a powerful by-product

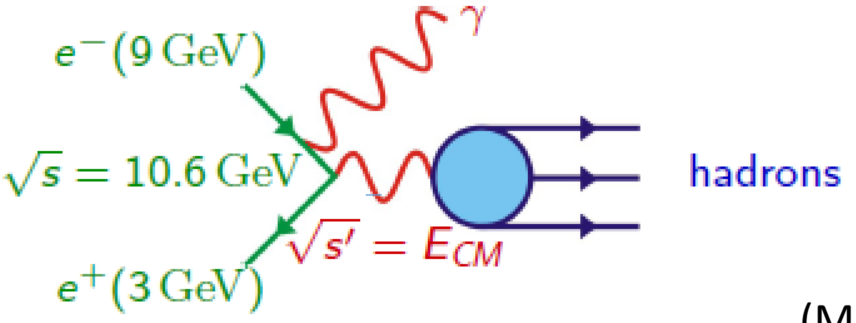

$$x = 2E^*_\gamma/\sqrt{s}$$

$$s' = s(1-x)$$

($M^2_{hadrons}$)

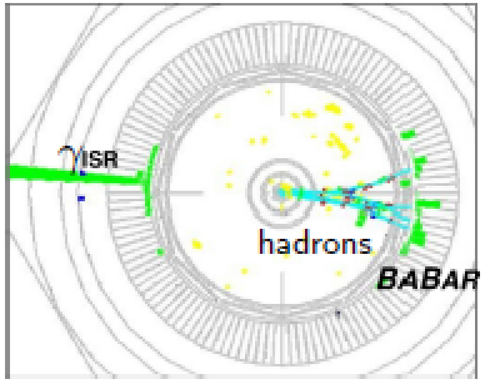

- High energy (E^*_γ >3 GeV) detected at large angle
- Event topology: ISR photon back-to-back to hadrons → high acceptance
- Final state can be hadronic or leptonic (QED)
  → $\mu^+\mu^-\gamma(\gamma)$ to get ISR luminosity
- Continuous measurement from threshold to 3-5 GeV
  →reduces systematic uncertainties compared to multiple data sets with different colliders and detectors

KKbar+π's Channels

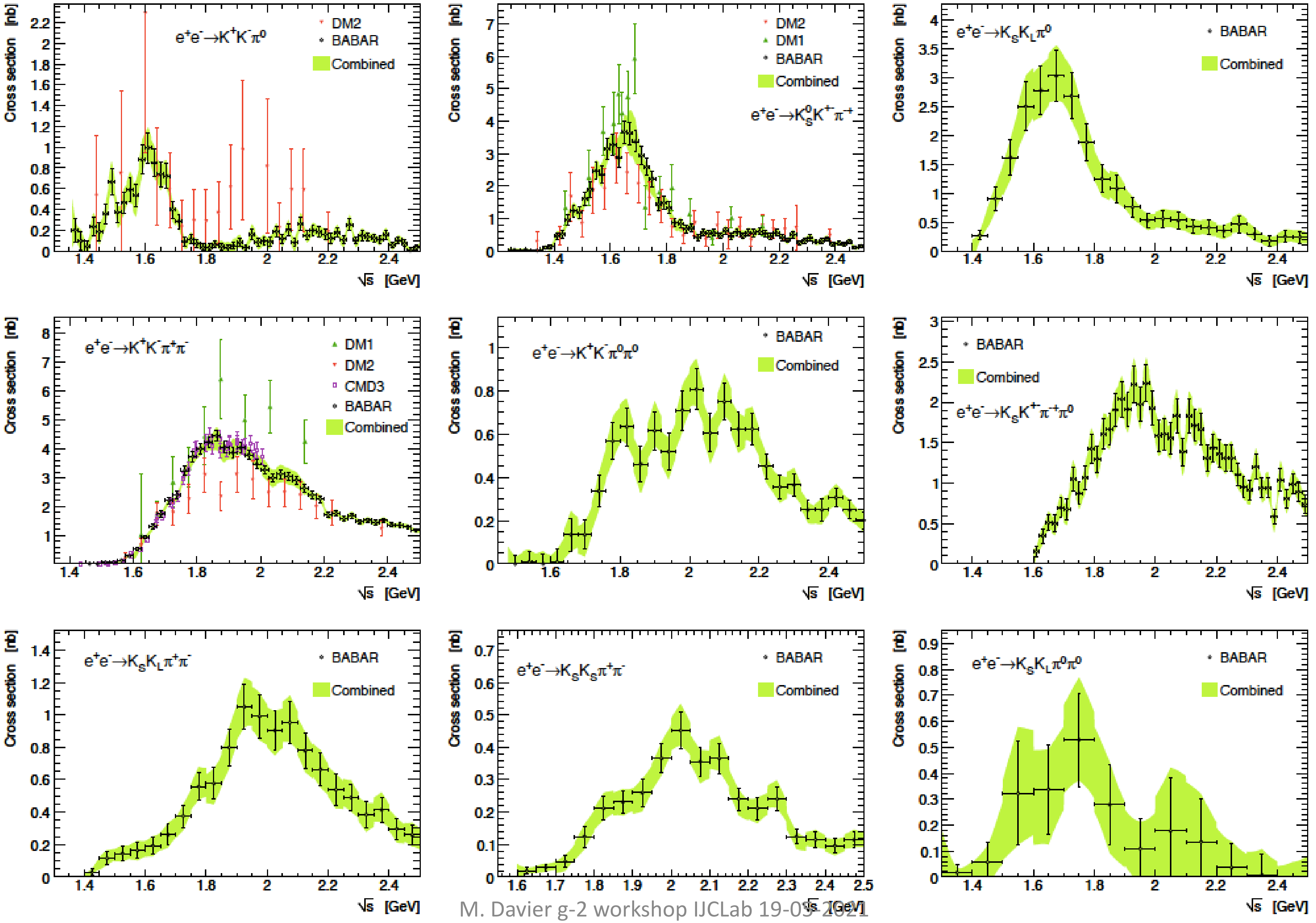

Contributions in the Region 1.8-3.7 GeV

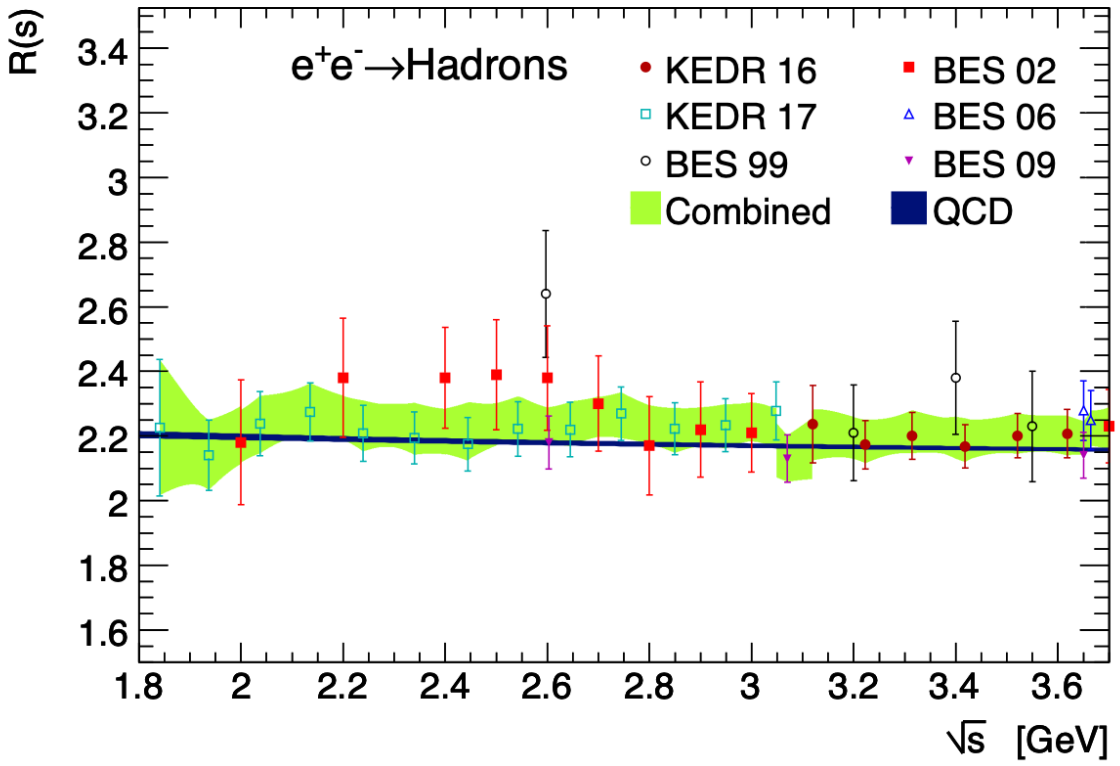

Energy range [GeV]	1.8 - 2.0	2.0 - 3.7
Data	7.71 ± 0.32	25.82 ± 0.61
pQCD	8.30 ± 0.09	25.15 ± 0.19
Difference	0.59 → dual	agree < 1σ

pQCD evaluated from 4 loops + $O(\alpha_s^2)$ quark mass corrections

Uncertainties: α_s, truncation, FOPT/CIPT, m_q

Contributions from Charm Resonance Region

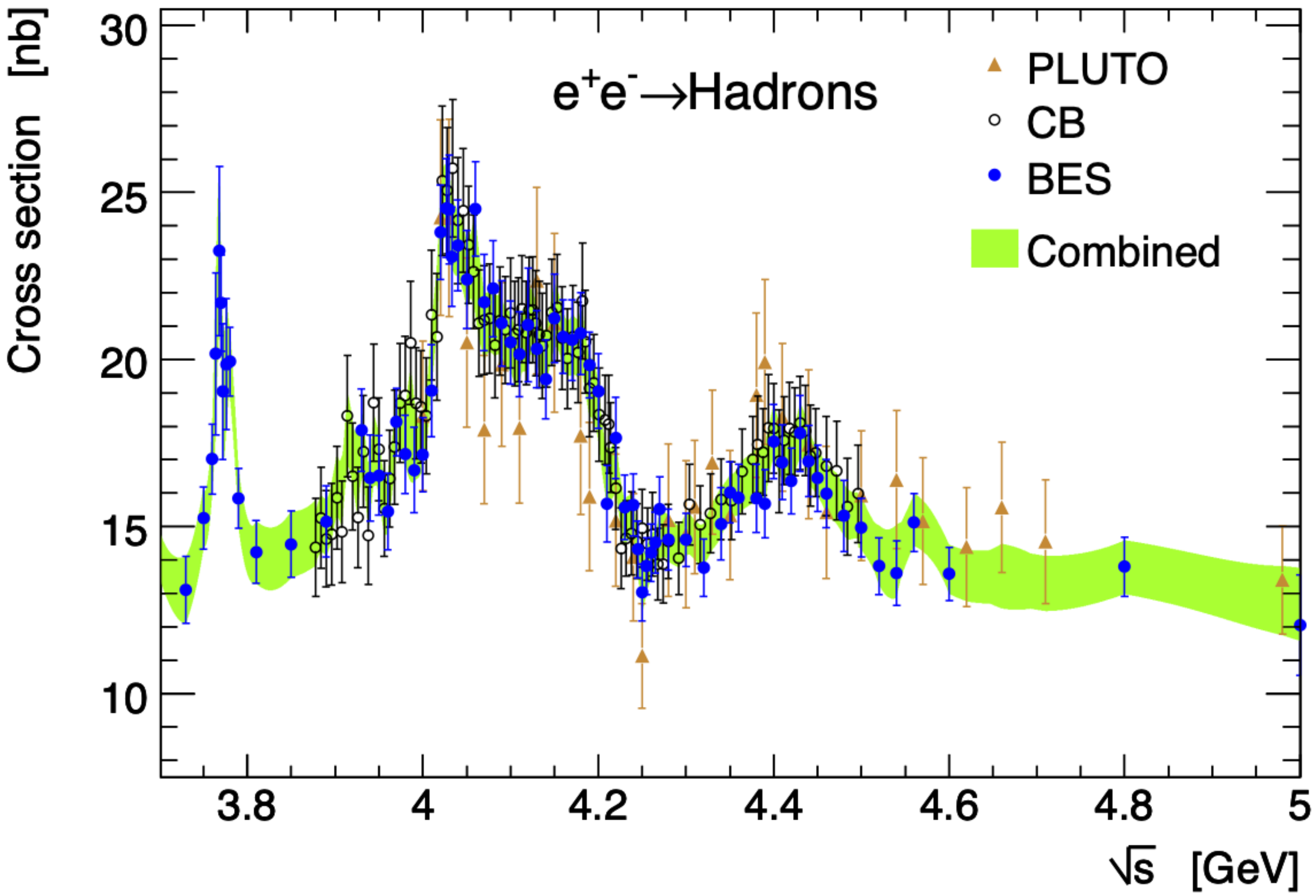

$7.29 \pm 0.05 \pm 0.30 \pm 0.00 \Rightarrow 1.05\%$ of $a_{\mu}^{\text{had, LO}}$

stat sys cor

An Alternative Way Used to Evaluate HVP

Proposed by Alemany-Davier-Hoecker, EPJC 2 (1998) 123

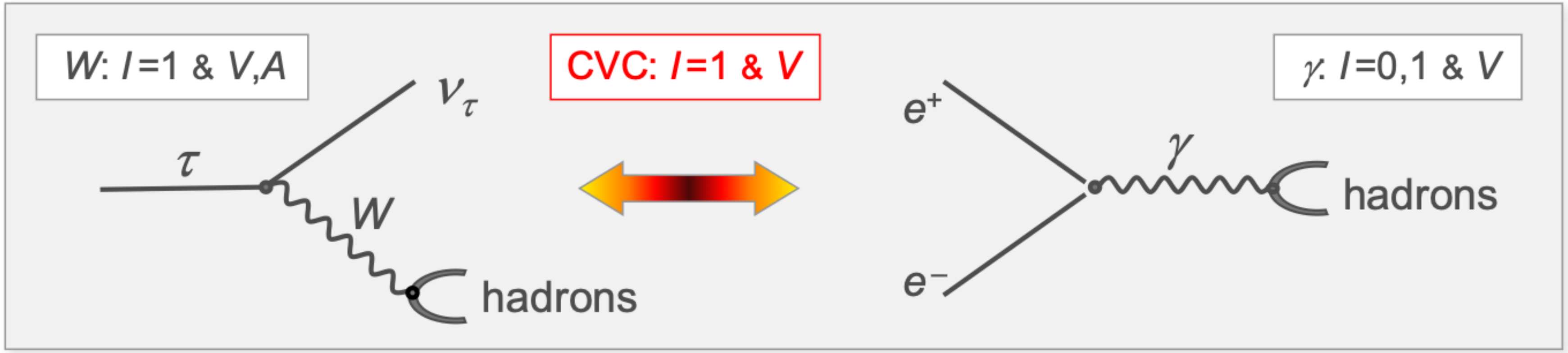

Hadronic physics factorises in Spectral Functions:
Isospin symmetry connects I=1 e^+e^- cross section to vector τ spectral functions

Fundamental ingredient relating long distance (resonances) to short distance description (QCD)

$$\sigma^{(I=1)}\left[e^+e^- \to \pi^+\pi^-\right] = \frac{4\pi\alpha^2}{s}\,\upsilon\left[\tau^- \to \pi^-\pi^0\nu_\tau\right]$$

$$\upsilon\left[\tau^- \to \pi^-\pi^0\nu_\tau\right] \propto \frac{BR\left[\tau^- \to \pi^-\pi^0\nu_\tau\right]}{BR\left[\tau^- \to e^-\bar{\nu}_e\nu_\tau\right]} \frac{1}{N_{\pi\pi^0}}\frac{dN_{\pi\pi^0}}{ds} \frac{m_\tau^2}{\left(1-s/m_\tau^2\right)^2\left(1+s/m_\tau^2\right)}$$

Branching fractions — Mass spectrum — Kinematic factors (PS)

Known Isospin Breaking Corrections

Davier et al., EPJC66 (2010) 127

$$v_{1,X^-}(s) = \frac{m_\tau^2}{6|V_{ud}|^2}\frac{\mathcal{B}_{X^-}}{\mathcal{B}_e}\frac{1}{N_X}\frac{dN_X}{ds} \times \left(1-\frac{s}{m_\tau^2}\right)^{-2}\left(1+\frac{2s}{m_\tau^2}\right)^{-1}\frac{R_{IB}(s)}{S_{EW}},$$

$$R_{IB}(s) = \frac{FSR(s)}{G_{EM}(s)}\frac{\beta_0^3(s)}{\beta_-^3(s)}\left|\frac{F_0(s)}{F_-(s)}\right|^2$$

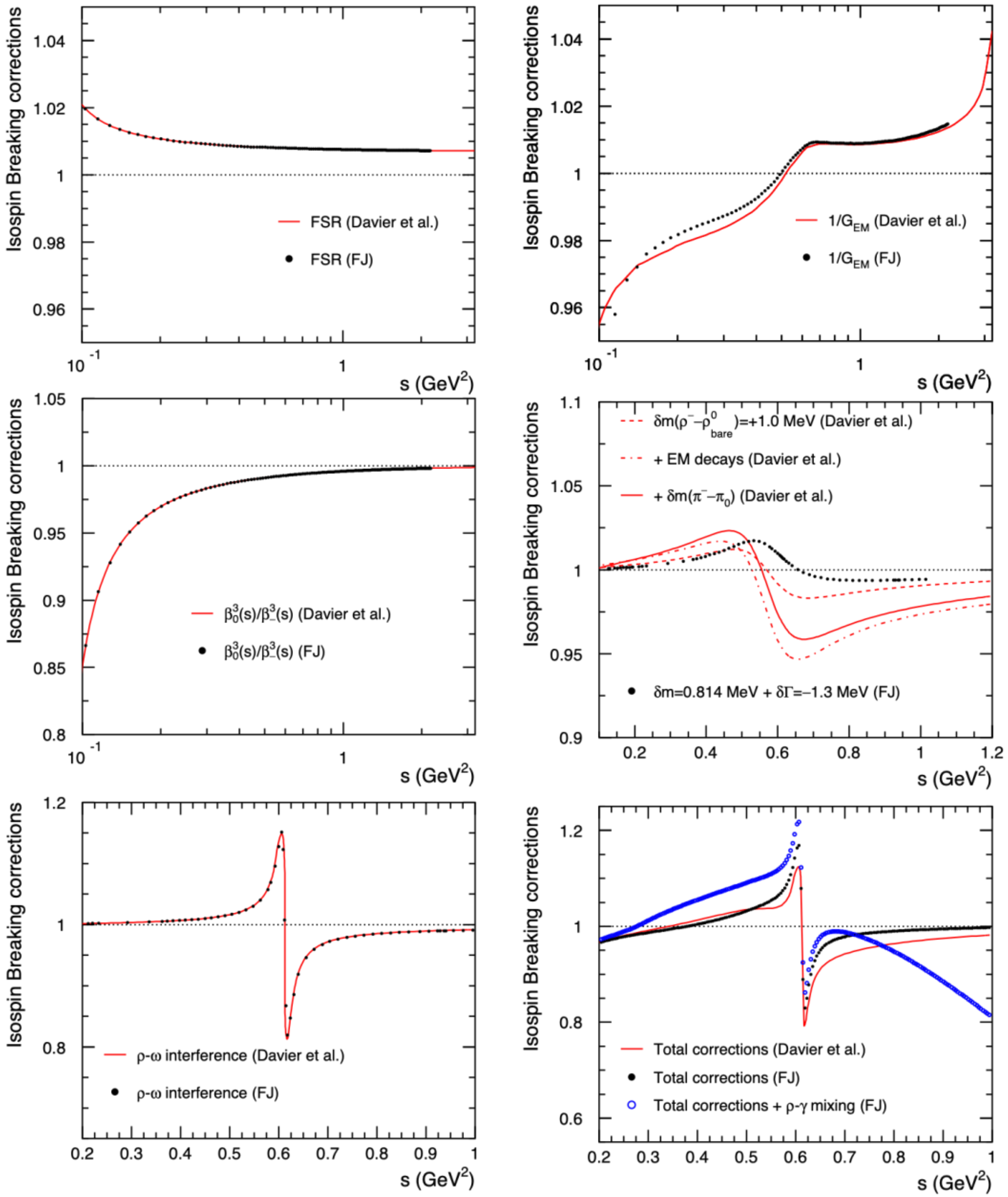

Good agreement between Davier et al. and FJ for most of the isospin breaking components

Figure 19 from WP20
Studies in DHMZ et al., EPJC66 (2010) 127

Open Issue in the 2π Channel

Take into account all known isospin breaking corrections except for the ρ–γ mixing correction

DHMYZ, EPJC66 (2010) 1

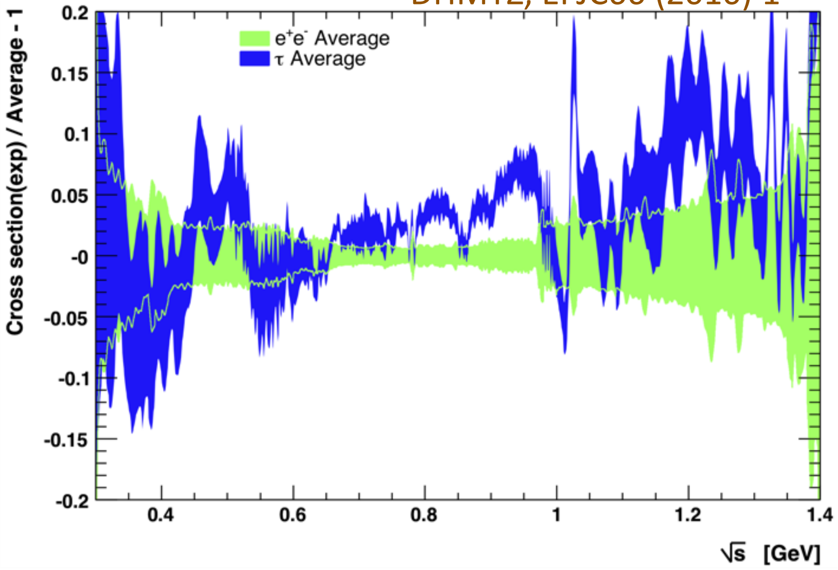

$$\mathcal{B}_X^{\rm CVC} = \frac{3}{2}\frac{\mathcal{B}_e |V_{ud}|^2}{\pi\alpha^2 m_\tau^2}\int_{s_{\rm min}}^{m_\tau^2} ds\, s\, \sigma_{X^0}^I \left(1-\frac{s}{m_\tau^2}\right)^2\left(1+\frac{2s}{m_\tau^2}\right)$$

Modified version from Davier et al,, EPJC66 (2010) 127

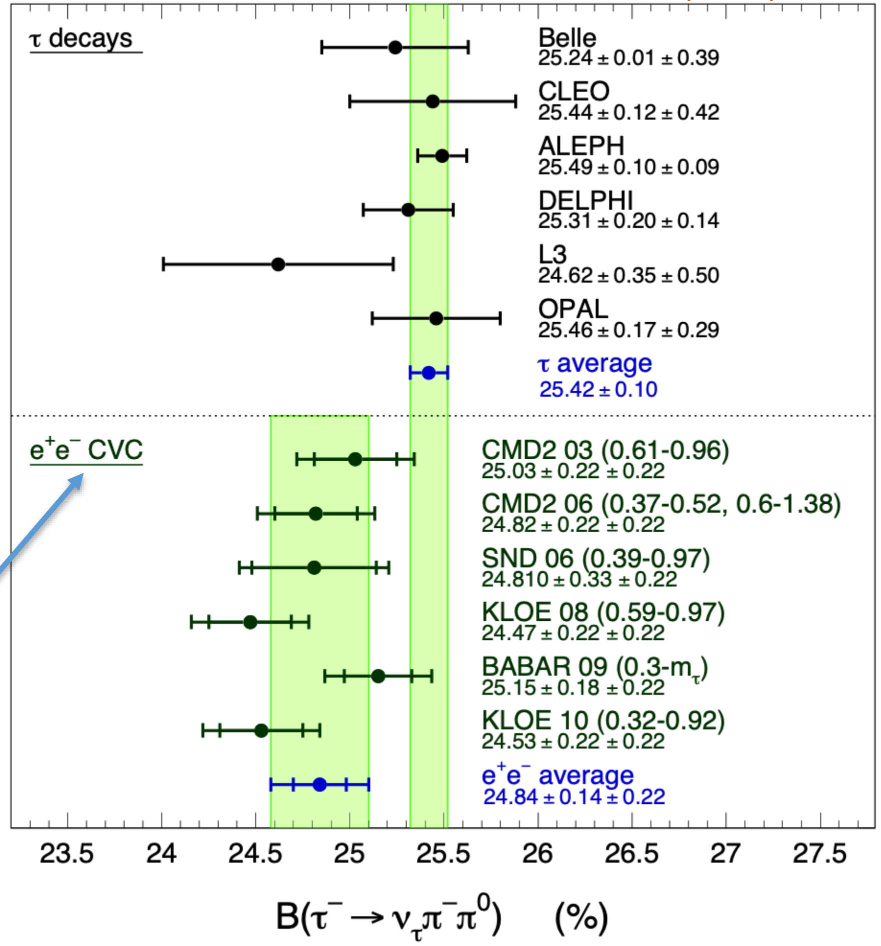

Clear difference in shape and in BR between e^+e^- and τ average

Additional EFT Based $\rho-\gamma$ Mixing Correction

JS, EPJC71 (2011) 1632

Jegerlehner and Szafron argue for a $\rho-\gamma$ mixing contribution in e+e- data, missing in τ data (problematic)

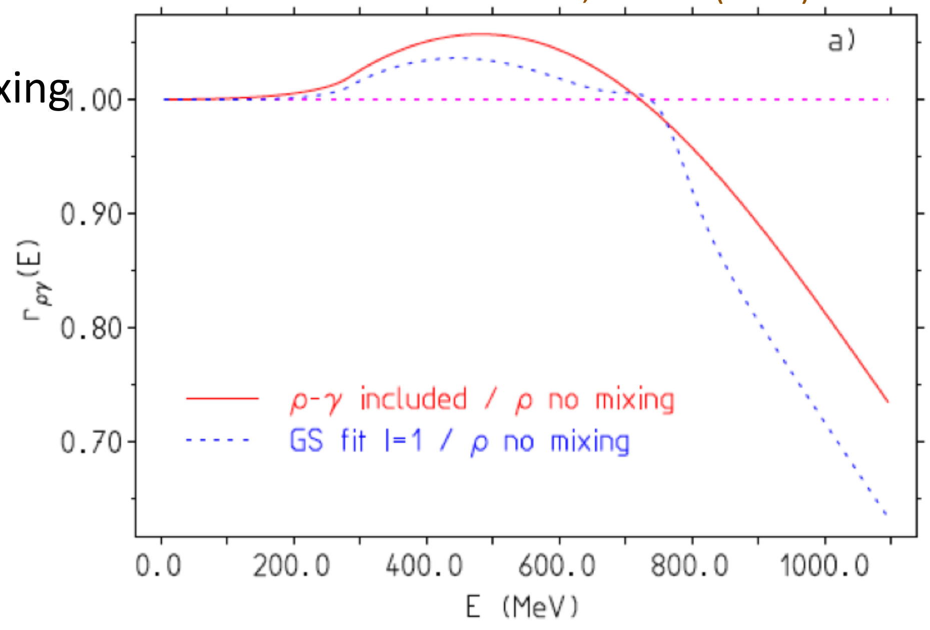

Figure 22 from WP20

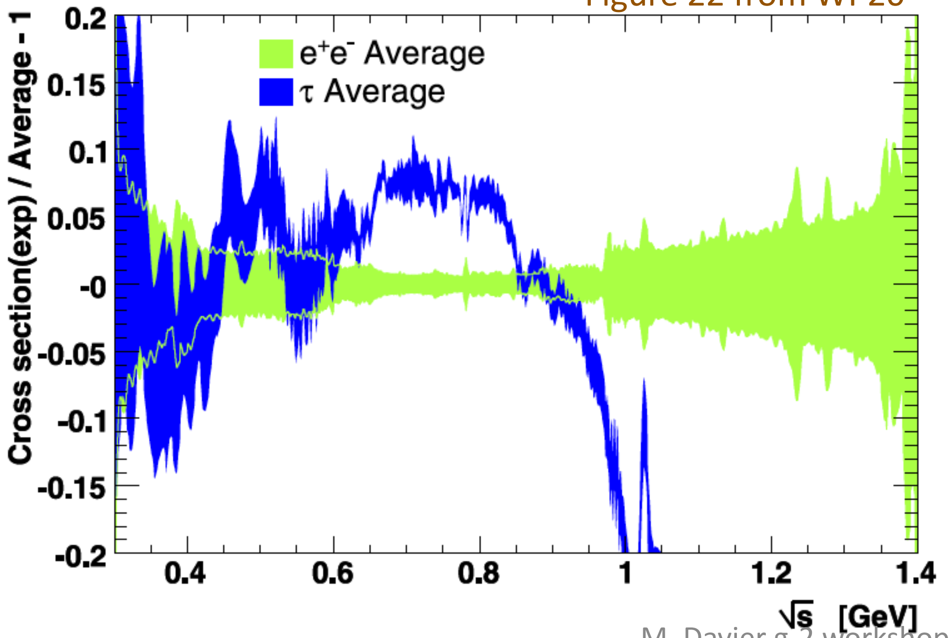

Applying the $\rho-\gamma$ mixing correction makes the e^+e^- and τ difference worse in some of the mass range